

Phonon coupling effects in magnetic moments of magic and semi-magic nuclei

E. E. Saperstein

Kurchatov Institute, 123182 Moscow

O. Achakovskiy and S. Kamedzhiev

Institute for Physics and Power Engineering, 249033 Obninsk, Russia

S. Krewald and J. Speth

Institut für Kernphysik, Forschungszentrum Jülich, D-52425 Jülich, Germany

S. V. Tolokonnikov

Kurchatov Institute, 123182 Moscow and

Moscow Institute of Physics and Technology, 141700 Dolgoprudny, Russia.

Phonon coupling (PC) corrections to magnetic moments of odd neighbors of magic and semi-magic nuclei are analyzed within the self-consistent Theory of Finite Fermi Systems (TFFS) based on the Energy Density Functional by Fayans *et al.* The perturbation theory in g_L^2 is used where g_L is the phonon-particle coupling vertex. A model is developed with separating non-regular PC contributions, the rest is supposed to be regular and included into the standard TFFS parameters. An ansatz is proposed to take into account the so-called tadpole term which ensures the total angular momentum conservation with g_L^2 accuracy. An approximate method is suggested to take into account higher order terms in g_L^2 . Calculations are carried out for four odd-proton chains, the odd Tl, Bi, In and Sb ones. Different PC corrections strongly cancel each other. In the result, the total PC correction to the magnetic moment in magic nuclei is, as a rule, negligible. In non-magic nuclei considered it is noticeable and, with only one exception, negative. On average it is of the order of $-(0.1 \div 0.5) \mu_N$ and improves the agreement of the theory with the data. Simultaneously we calculated the gyromagnetic ratios g_L^{ph} of all low-lying phonons in ^{208}Pb . For the 3_1^- state it is rather close to the Bohr–Mottelson model prediction whereas for other L -phonons, two 5^- and six positive parity states, the difference from the Bohr–Mottelson values is significant.

PACS numbers: 21.60.Jz, 21.10.Ky, 21.10.Ft, 21.10.Re

I. INTRODUCTION

This work is devoted to studying effects of the interaction of low-lying collective states (“phonons”) with single-particle degrees of freedom. The first microscopic description of phonons in spherical nuclei was made more than 50 years ago by Spartak Belyaev in the seminal article [1].

In the last decade, a considerable success of different approaches based on the mean field theory in the description of nuclear bulk properties was achieved. It concerns the Hartree–Fock (HF) method with Skyrme force [2, 3], the HF method with Gogny force [4], the Relativistic Mean-Field approach [5] and the so-called Generalized Energy Density Functional (EDF) method by Fayans *et al.* [6]. The last approach is essentially close to the self-consistent Theory of Finite Fermi Systems (TFFS) [7] based on TFFS by Migdal [8] supplemented with the Fayans–Khodel self-consistency relation [9]. A specific feature of the Fayans method is the consideration of the pairing problem by solving the Gor’kov equations in the coordinate space with the method developed by Belyaev *et al.* [10]. Recently, all these approaches were also successfully applied to the description of phonons in spherical nuclei within the self-consistent Quasiparticle Random Phase Approximation (QRPA) or similar methods,

see e.g. [11–15].

The next step consists in taking into account the phonon coupling (PC) effects. These effects were studied in detail in the Quasiparticle-Phonon Model by Soloviev [16] and, on the phenomenological level, within the so-called Nuclear Field Theory by Bortignon, Broglia *et al.* [17]. On a more microscopic level, they were considered mainly for describing different kinds of Giant Resonances and the Pygmy-dipole Resonance within the (Q)RPA+PC method [18] and Extended Theory of Finite Fermi Systems (ETFFS) [19]. Self-consistent extensions of these methods have been proposed recently, for example, (Q)RPA+PC [20] and the ETFFS in the Quasiparticle Time Blocking Approximation (QTBA) [21] [ETFFS(QTBA)] [22], see also the recent review [23] devoted to the Pygmy-dipole Resonance. It should be mentioned as well successful applications of the self-consistent ETFFS(QTBA) in [24] and in [25]. The approach is limited to magic and semi-magic nuclei where there is a small parameter g_L^2 , the square of the phonon creation amplitude.

Here we concentrate on the self-consistent description of the PC corrections to magnetic moments. Due to modern Radioactive Ion Beam facilities a lot of new data on magnetic and quadrupole moments appeared recently including nuclei distant from the beta-decay valley. The

bulk of the data obtained till 2005 is collected in a very comprehensive compilation by Stone [26]. More recent data are presented in original articles, e.g. in Ref. [27], where new, together with older, data on magnetic and quadrupole moments of a long chain of copper isotopes from $N = 28$ to $N = 46$ are presented and successfully analyzed within the Many-Particle Shell Model (MPSM) [28]. This approach is very comprehensive as it takes into account all main inter-nuclear correlations. The necessity to introduce many parameters of the effective interaction, the single-particle mean field and the effective particle charges is some deficiency of the MPSM. In addition, the domain of the MPSM applications is, by technical reasons, limited to nuclei with $A < 90 \div 100$.

For heavier nuclei, the challenge of experimentalists was partially responded within the self-consistent TFFS for magnetic moments [29, 30] and quadrupole moments [15, 31, 32] of odd spherical nuclei. Mention also the first self-consistent calculation of the quadrupole moments of the 2_1^+ states [33]. The calculations were mainly limited to semi-magic nuclei considered in the “single-quasiparticle approximation” where one quasiparticle in the fixed state $\lambda = (n, l, j, m)$ with the energy ε_λ is added to the even-even core. The QRPA-like TFFS equations for the nuclear response to the external field, magnetic in [29, 30] or quadrupole in [15, 31, 32], were solved on the base of the Energy Density Functional (EDF) by Fayans et al. [6, 34, 35]. For magnetic moments, the original Fayans functional DF3 [6, 35] was used whereas for quadrupole moments it was used together with its modification, DF3-a, which was introduced in [36] to extend this approach to nuclei heavier than lead. It differs from the original one by the spin-orbit and effective tensor terms which are important only for the fine structure of the single-particle spectrum. For the quadrupole moments, the difference between the predictions of the two functionals turned out noticeable with a preference of DF3-a. We also mention that the same is true for the energies and excitation probabilities of the 2_1^+ states in the lead and tin isotopes [15, 37].

According to the TFFS [8], a quasiparticle differs from a particle of the single-particle model in two respects. First, it possesses a local charge e_q and, second, the core is polarized due to the interaction between the particle and the core nucleons via the Landau-Migdal (LM) amplitude \mathcal{F} . In other words, the quasiparticle possesses the effective charge e_{eff} caused by the polarizability of the core which is found by solving the TFFS equations. In the MPSM, a similar quantity is introduced as a phenomenological parameter. Thus, the consideration was made on the RPA (or QRPA) level which is the “zero approximation” to the problem, corrections due to phonon coupling (PC) effects were only estimated in [29–31]. This does not concern the investigation of quadrupole moments of the 2_1^+ states in Ref. [33] as the effect under consideration there is beyond QRPA itself. On average, reasonable description of the data was obtained in the Refs. cited above, with the accuracy

of $\delta\mu \simeq 0.1 \div 0.2$ n.m. for magnetic moments, and $\delta Q \simeq 0.1 \div 0.2$ b for quadrupole moments. This indicates that the single-quasiparticle approximation works well for such nuclei on average, and the PC effects are usually regular and included in the TFFS parameters, i.e. the charges e_q and the LM amplitudes \mathcal{F} . However, there are several “bad” cases, with $\delta\mu \simeq 0.5$ n.m. for magnetic moments, and $\delta Q \simeq 0.5$ b for quadrupole moments which were attributed to some non-regular PC effects. The estimations in [30] for magnetic moments and in [31] for quadrupole ones have shown that this interpretation looks reasonable and a more detailed analysis of the PC effects is necessary.

In this context, it is worth citing older calculations of magnetic moments within the conventional TFFS with the use of the Saxon-Woods potential as the nuclear mean field [38–40].

Dealing with the PC problem within TFFS or other microscopic approaches with fitted parameters, one faces the problem of refitting the parameters provided all the PC corrections are taken into account. Exactly this way was chosen in [24], where a new set parameters of the Skyrme functional was found which corrects for the PC effects. The same mode of action was used in the first version of the self-consistent TFFS [7]. In this paper, dealing with magnetic moments of magic and semi-magic nuclei, we chose a simpler way by separating only the kinds of the PC diagrams which behave in non-regular way depending significantly on the nucleus and the single-particle state under consideration. The rest of the PC corrections, in agreement with the estimations, is supposed to be regular and is included in the standard TFFS parameters. Within this model, we analyzed first odd neighbors of the magic ^{208}Pb nucleus. In this case the PC effects appear mainly due to the 3_1^- state, although sometimes the sum of contributions of all other phonons is also important. For these nuclei, the problem was analyzed in the well-known paper by I. Hamamoto [41] within the Nuclear Field Theory [17], the approach which operates with a set of phenomenological parameters for each nucleus under consideration. On a microscopic level, this problem was considered by Platonov [42] and Tselyaev [43]. In the last article, some sets of higher order terms in g_L^2 were summed up within QTBA.

In non-magic nuclei, the contribution of the 2_1^+ state dominates. Again we limit ourselves to the semi-magic nuclei where this state is usually not too collective and the parameter g_L^2 is, as a rule, small. In addition, we will consider only such odd semi-magic nuclei where the odd nucleon belongs to the normal sub-system which simplifies the calculations because all the equations for the PC corrections do not include pairing effects. For example, in the lead region we will analyze the odd Tl and Bi isotopes, but not the odd Pb nuclei, except $^{207,209}\text{Pb}$.

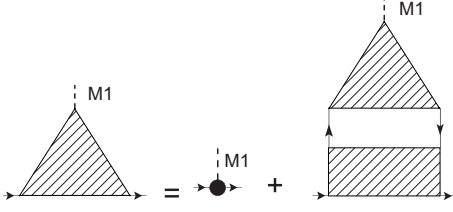


FIG. 1: The effective magnetic field $V(M1)$. The meaning of separate blocks becomes obvious after comparing with Eq. (2).

II. SELF-CONSISTENT TFFS

For completeness, we outline first the TFFS formalism for the effective magnetic field without phonon corrections. The magnetic moment of an odd nucleus or the probability of the $M1$ -transition in such a nucleus are determined from the effective field V which is related to the external field $V_0 = \hat{\mu}$, where $\hat{\mu}$ is the operator of the magnetic moment:

$$\hat{\mu} = g_l \hat{\mathbf{l}} + \frac{1}{2} g_s \hat{\boldsymbol{\sigma}}, \quad (1)$$

with $g_l^p=1$, $g_l^n=0$, $g_s^p=5.586$, and $g_s^n=-3.826$. The effective field V obeys an equation which is similar to the RPA equation with the LM amplitude \mathcal{F} playing the role of the effective NN-interaction. In systems without pairing, e.g. magic nuclei, this equation reads

$$V(M1; \omega) = V_0(M1) + \mathcal{F} A(\omega) V(M1; \omega), \quad (2)$$

where $V_0(M1) = e_q \hat{\mu}$ and $A(\omega) = \int G(\varepsilon) G(\varepsilon + \omega) d\varepsilon / (2\pi i)$ stands for the particle-hole propagator, $G(\varepsilon)$ being the single-particle Green function. This is illustrated diagrammatically on Fig. 1. The magnetic moments of an odd nucleus with the odd nucleon in the one-quasiparticle state $\lambda = (n_r, l, j, m) = (\nu, m)$ are the diagonal matrix elements of the static effective field, $\mu_\lambda = \langle \lambda | V(M1; \omega = 0) | \lambda \rangle_{m=j}$, whereas the matrix elements of the $M1$ -transition $\lambda_1 \rightarrow \lambda_2$ between two states with the energies ε_1 and ε_2 respectively are given by the non-diagonal matrix elements $M_{12} = \langle \lambda_1 | V(M1; \omega = \varepsilon_2 - \varepsilon_1) | \lambda_2 \rangle$.

In the explicit form, the local quasiparticle charge e_q in Eq. (2) is defined as follows:

$$\begin{aligned} e_q \hat{\mu} = & \frac{1 + (1 - 2\zeta_l) \hat{\tau}_3}{2} \hat{\mathbf{l}} \\ & + \frac{(g_s^p + g_s^n) + (g_s^p - g_s^n)(1 - 2\zeta_s) \hat{\tau}_3}{4} \hat{\boldsymbol{\sigma}} \\ & + \zeta_t [Y_2(\mathbf{n}) \otimes \hat{\boldsymbol{\sigma}}]^1. \end{aligned} \quad (3)$$

Here, following Refs.[29, 30], in addition to the usual local charge parameters ζ_s, ζ_l of the FFS theory [8], a

new “tensor” (or “ l -forbidden”) charge ζ_t is introduced. Terms of similar structure appear naturally from MEC contributions to the magnetic moments [44].

In nuclei with pairing, Eq. (2) transforms to a set of three equations [8]

$$\hat{V}(\omega) = \hat{V}_0(\omega) + \hat{\mathcal{F}} \hat{A}(\omega) \hat{V}(\omega), \quad (4)$$

where all the terms are matrices. In the standard TFFS notation [8], we have:

$$\hat{V} = \begin{pmatrix} V \\ d_1 \\ d_2 \end{pmatrix}, \quad \hat{V}_0 = \begin{pmatrix} V_0 \\ 0 \\ 0 \end{pmatrix}, \quad (5)$$

where the fields $d_{1,2}$ denote variations of the gap functions $\Delta^{(1,2)}$ in the external field V_0 . The vector analogue of (2) contains $3 \otimes 3$ matrices:

$$\hat{\mathcal{F}} = \begin{pmatrix} \mathcal{F} & \mathcal{F}^{\omega\xi} & \mathcal{F}^{\omega\xi} \\ \mathcal{F}^{\xi\omega} & \mathcal{F}^\xi & \mathcal{F}^{\xi\omega} \\ \mathcal{F}^{\xi\omega} & \mathcal{F}^{\xi\omega} & \mathcal{F}^\xi \end{pmatrix}, \quad (6)$$

and

$$\hat{A}(\omega) = \begin{pmatrix} \mathcal{L}(\omega) & \mathcal{M}_1(\omega) & \mathcal{M}_2(\omega) \\ \mathcal{O}(\omega) & -\mathcal{N}_1(\omega) & \mathcal{N}_2(\omega) \\ \mathcal{O}(-\omega) & -\mathcal{N}_1(-\omega) & \mathcal{N}_2(-\omega) \end{pmatrix}, \quad (7)$$

where \mathcal{L} , \mathcal{M}_1 , and so on stand for integrals over ε of the products of different combinations of the Green function $G(\varepsilon)$ and two Gor'kov functions $F^{(1)}(\varepsilon)$ and $F^{(2)}(\varepsilon)$ [8].

In the matrix $\hat{\mathcal{F}}$, the diagonal terms are the usual LM amplitude \mathcal{F} of the effective interaction in the particle-hole (ph) and the interaction amplitude \mathcal{F}^ξ irreducible in the pp (or hh) channel. The non-diagonal terms couple the ph channel with the pp and hh ones. As the analysis of [29] has shown, the interaction amplitude \mathcal{F}^ξ for the $M1$ symmetry is, evidently, small. Therefore, we put $\mathcal{F}^\xi=0$. Then, it is natural also to put equal to zero all the non-diagonal terms of \mathcal{F}^ξ . In this case, we have $d_1 = d_2 = 0$ and the only modification of Eq. (2) is the change $A \rightarrow \mathcal{L}$,

$$\mathcal{L}(\omega) = \int \frac{d\varepsilon}{2\pi i} \left[G(\varepsilon) G(\varepsilon + \omega) - F_1(\varepsilon) F_2(\varepsilon + \omega) \hat{P} \right], \quad (8)$$

where $\hat{P} = 1$ for T-even fields and $\hat{P} = -1$ for the T-odd ones. To calculate the propagator \mathcal{L} with consistent account for the continuum states, we use the generalization [45] for superfluid systems of the Shlomo-Bertsch method [46].

All calculations below will be carried out with the use of the self-consistent basis generated with the Generalized EDF by Fayans et al.,

$$E_0 = \int \mathcal{E}[\rho_n(\mathbf{r}), \rho_p(\mathbf{r}), \nu_n(\mathbf{r}), \nu_p(\mathbf{r})] d^3r, \quad (9)$$

depending simultaneously on the normal ρ_τ and anomalous ν_τ densities. The DF3-a version of the normal EDF

[36] will be used and the “surface” anomalous EDF [6]. More details can be found in [15].

For magnetic moments we consider only the spin-dependent parameters contribute. The spin-dependent LM amplitude, just as in [29, 30], is chosen in the form of

$$\mathcal{F}^{\text{spin}} = \mathcal{F}_0^{\text{spin}} + \mathcal{F}_\pi + \mathcal{F}_\rho, \quad (10)$$

where the pion and ρ -meson exchange terms are added to the central force term \mathcal{F}_0 . The central force was approximated with the zero Landau harmonics. Following to [47, 48], we take into account the momentum dependence of the amplitude g' (“Migdal force”):

$$\mathcal{F}_0^{\text{spin}} = C_0 [g(\boldsymbol{\sigma}_1 \boldsymbol{\sigma}_2) + g'(q)(\boldsymbol{\sigma}_1 \boldsymbol{\sigma}_2)(\boldsymbol{\tau}_1 \boldsymbol{\tau}_2)], \quad (11)$$

$$g'(q) = \frac{g'}{1 + r_0^2 q^2}, \quad (12)$$

where the normalization factor $C_0 = dn/d\varepsilon_F)^{-1} = 300 \text{ MeV} \cdot \text{fm}^3$, and the value of $r_0 = 0.4 \text{ fm}$ was found in [47, 48] for the parameter which determines the dependence of the amplitude g' on the momentum transfer.

To evaluate the PC corrections we need in the vertex $\hat{g}_L(r)$, the creation amplitude of the L -phonon. It obeys the homogeneous equation corresponding to Eq. (4),

$$\hat{g}_L(\omega) = \hat{\mathcal{F}} \hat{A}(\omega) \hat{g}_L(\omega), \quad (13)$$

and is normalized as follows [8],

$$\left(\hat{g}_L^+ \frac{d\hat{A}}{d\omega} \hat{g}_L \right)_{\omega=\omega_L} = -1, \quad (14)$$

with the following notation:

$$\hat{g}_L = \begin{pmatrix} g_L^{(0)} \\ g_L^{(1)} \\ g_L^{(2)} \end{pmatrix}, \quad (15)$$

All the low-lying phonons we will consider have natural parity. In this case, the vertex \hat{g}_L possesses even T -parity. It is a sum of two components with spins $S = 0$ and $S = 1$, respectively:

$$\hat{g}_L = \hat{g}_{L0}(r) T_{LL0}(\mathbf{n}, \alpha) + \hat{g}_{L1}(r) T_{LL1}(\mathbf{n}, \alpha), \quad (16)$$

where T_{JLS} stand for the usual spin-angular tensor operators [49]. The operators T_{LL0} and T_{LL1} have opposite T -parities, hence the spin component should be the odd function of the excitation energy, $g_L^{(1)} \propto \omega_L$. In this case, the LM amplitude in Eq. (13) is also the sum,

$$\mathcal{F} = \mathcal{F}_0 + \mathcal{F}^{\text{spin}}, \quad (17)$$

where the spin-independent LM amplitude is generated by the generalized EDF in Eq. (9),

$$\mathcal{F}_0 = \frac{\delta^2 \mathcal{E}}{\delta \rho^2}. \quad (18)$$

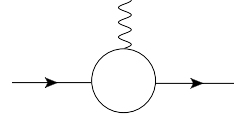


FIG. 2: The L -phonon creation amplitude $g_L(\mathbf{r})$.

The non-diagonal components of the matrix (6), the amplitudes $\mathcal{F}^{\omega\xi} = \mathcal{F}^{\xi\omega}$ stand for the mixed second derivatives,

$$\mathcal{F}^{\omega\xi} = \frac{\delta^2 \mathcal{E}}{\delta \rho \delta \nu}, \quad (19)$$

and, finally, the amplitude \mathcal{F}^ξ is the effective pairing interaction entering the gap equation,

$$\Delta = \mathcal{F}^\xi \nu. \quad (20)$$

The isotopic indices in Eqs. (13 – 20) are for brevity omitted. In the case of the surface pairing we deal, the “mixed” amplitude $\mathcal{F}^{\omega\xi}$ is rather important for the correct solution of the self-consistent QRPA equation (13).

III. PC CORRECTIONS IN MAGIC AND SEMI-MAGIC NUCLEI

Let us now consider the PC corrections to Eq. (2) induced by a L -phonon. Keeping in mind the smallness of the g_L^2 parameter, we limit ourselves to the so-called g_L^2 -approximation. In addition, as it was mentioned in the Introduction, we limit ourselves with the case where the odd nucleon belongs to the non-superfluid sub-system. We will consider mainly the PC corrections for this sub-system, therefore the component $g_L^{(0)}$ of the vector (15) will participate only. To shorten notation, we will omit for a time the upper index putting $g_L^{(0)} \rightarrow g_L$. To be more exact, we deal with the PC corrections to the matrix element $V_{\lambda_2 \lambda_1} = (\phi_{\lambda_2}, V(M1) \phi_{\lambda_1})$ which is the second order variation in the phonon field g_L , see Fig. 2,

$$\begin{aligned} \delta^{(2)} V_{\lambda_2 \lambda_1} &= (\delta^{(2)} \phi_{\lambda_2}, V \phi_{\lambda_1}) + (\phi_{\lambda_2}, V \delta^{(2)} \phi_{\lambda_1}) \\ &+ (\delta^{(1)} \phi_{\lambda_2}, V \delta^{(1)} \phi_{\lambda_1}) + (\phi_{\lambda_2}, \delta^{(2)} V \phi_{\lambda_1}) \\ &+ (\delta^{(1)} \phi_{\lambda_2}, \delta^{(1)} V \phi_{\lambda_1}) + (\phi_{\lambda_2}, \delta^{(1)} V \delta^{(1)} \phi_{\lambda_1}), \end{aligned} \quad (21)$$

with the obvious notation. In the cases where it can not lead to misleading, we shorten the notation below as follows $\delta^{(2)} \rightarrow \delta$.

A. PC corrections included into the model

We separate those terms of Eq. (21) which may behave in non-regular way changing significantly depending on the nucleus and the state under considerations. As it

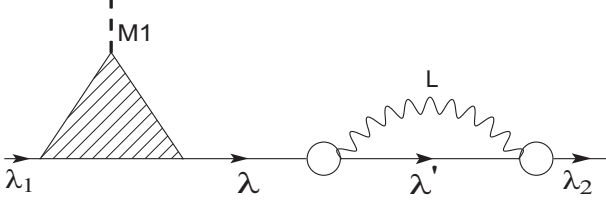


FIG. 3: A correction to the “end”. The open blob is the L -phonon creation amplitude $g_L(\mathbf{r})$. The wavy line denotes the phonon D -function.

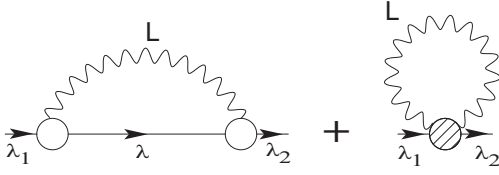


FIG. 4: PC corrections to the mass operator. The dashed blob denotes the “tadpole” term.

will be argued in the next subsection, this does concern the three first terms of Eq. (21). The last two terms disposed in the third line are regular and can be included into the TFFS parameters. As to the forth term, $\delta^{(2)}V$, it contains both, the regular and non-regular contributions.

The terms in the first line of (21), the second order variations of the single-particle wave functions may be named as the “end correction”, keeping in mind the ends of the diagram of Fig. 1 for the effective field. The main, pole part of the end correction corresponding to the second of these two terms is illustrated in Fig. 3. The corresponding tadpole term is shown in Fig. 4. The phonon D -function appears here and below after connecting two wavy ends of Fig. 2 which corresponds to averaging of the product of two boson (phonon) operators B^+B over the ground state of the nucleus without phonons.

For the matrix element $V_{\lambda_2\lambda_1}$ of the effective field, the sum of these corrections corresponds to the following formula:

$$\begin{aligned} \delta V_{\lambda_2\lambda_1}^{\text{end}} = & - \sum_{\lambda} V_{\lambda_2\lambda} G_{\lambda}(\varepsilon_{\lambda_1}) \delta \Sigma_{\lambda\lambda_1}(\varepsilon_{\lambda_1}) \\ & - \sum_{\lambda} \delta \Sigma_{\lambda_2\lambda}(\varepsilon_{\lambda_2}) G_{\lambda}(\varepsilon_{\lambda_2}) V_{\lambda\lambda_1}. \end{aligned} \quad (22)$$

Here $\delta \Sigma$ means the PC correction to the mass operator Σ displayed in Fig. 4. In addition to the pole diagram of Fig. 4, we showed also for completeness the non-pole “tadpole” one [7]. As we will see, this term $\delta \Sigma^{\text{tad}}$ does

practically not contribute to the problem under consideration.

The pole diagram in Fig. 4 corresponds to the following expression,

$$\begin{aligned} \delta \Sigma_{\lambda_2\lambda_1}(\varepsilon) = & \int \frac{d\omega}{2\pi i} \sum_{\lambda M} \langle \lambda_2 | g_{LM}^+ | \lambda \rangle \langle \lambda | g_{LM} | \lambda_1 \rangle \\ & \times D_L(\omega) G_{\lambda}(\varepsilon - \omega), \end{aligned} \quad (23)$$

where $D_L(\omega)$ is the phonon D -function. After an integration, one obtains

$$\begin{aligned} \delta \Sigma_{\lambda_2\lambda_1}(\varepsilon) = & \sum_{\lambda M} \langle \lambda_2 | g_{LM}^+ | \lambda \rangle \langle \lambda | g_{LM} | \lambda_1 \rangle \\ & \times \left(\frac{n_{\lambda}}{\varepsilon + \omega_L - \varepsilon_{\lambda}} + \frac{1 - n_{\lambda}}{\varepsilon - \omega_L - \varepsilon_{\lambda}} \right), \end{aligned} \quad (24)$$

where ω_L is the excitation energy of the L -phonon and $n_{\lambda} = (0, 1)$ stands for the occupation numbers.

After substitution of (24) into (22) one obtains:

$$\begin{aligned} \delta V_{\lambda_2\lambda_1}^{\text{end}} = & - \sum_{\lambda' \lambda M} \frac{V_{\lambda_2\lambda} \langle \lambda | g_{LM}^+ | \lambda' \rangle \langle \lambda' | g_{LM} | \lambda_1 \rangle}{\varepsilon_{\lambda_1} - \varepsilon_{\lambda}} \\ & \times \left(\frac{n_{\lambda'}}{\varepsilon_{\lambda_1} + \omega_L - \varepsilon_{\lambda'}} + \frac{1 - n_{\lambda'}}{\varepsilon_{\lambda_1} - \omega_L - \varepsilon_{\lambda'}} \right) \\ & - \sum_{\lambda \lambda' M} \left(\frac{n_{\lambda'}}{\varepsilon_{\lambda_2} + \omega_L - \varepsilon_{\lambda'}} + \frac{1 - n_{\lambda'}}{\varepsilon_{\lambda_2} - \omega_L - \varepsilon_{\lambda'}} \right) \\ & \times \frac{\langle \lambda_2 | g_{LM}^+ | \lambda' \rangle \langle \lambda' | g_{LM} | \lambda \rangle V_{\lambda\lambda_1}}{\varepsilon_{\lambda_2} - \varepsilon_{\lambda}}. \end{aligned} \quad (25)$$

In this equation, the term with $\lambda = \lambda_1$ in the first sum and the one with $\lambda = \lambda_2$ in the second sum are singular. This singularity is removed with the standard renormalization [7] of the single particle wave functions $\varphi_{\lambda_1} \rightarrow \sqrt{Z_{\lambda_1}} \varphi_{\lambda_1}$, $\varphi_{\lambda_2} \rightarrow \sqrt{Z_{\lambda_2}} \varphi_{\lambda_2}$, where

$$Z_{\lambda} = \left(1 - \left. \frac{\partial \Sigma_{\lambda\lambda}(\varepsilon)}{\partial \varepsilon} \right|_{\varepsilon=\varepsilon_{\lambda}} \right)^{-1} \quad (26)$$

is the residue of the Green function at the pole $\varepsilon = \varepsilon_{\lambda}$.

To avoid misleading, we note that below we will for brevity name “ Z -factor” not the total quantity but the PC contribution only. Correspondingly, we insert into Eq. (26) the PC term $\delta \Sigma$ only. In the TFFS the total Z -factor enters into the LM amplitude $\mathcal{F} = Z^2 \Gamma^{\omega}$, the local charges $e_q = Z \mathcal{T}^{\omega}$ and the mean field $U(r) = Z \Sigma_0(r)$, where the subscript “0” means that the energy and momentum are taken at the Fermi surface. Here the notation [8] is used with the only change $a \rightarrow Z$. The average value of the Z -factor corresponding to the total mass operator Σ_0 was estimated in [7] and [50, 51] as $Z_0 = 0.8$.

The rest of these sums with non-diagonal terms $\lambda \neq \lambda_1$ in the first case and $\lambda \neq \lambda_2$ in the second can be calculated directly and, as we shall see, are rather small. However, we retain them for completeness, and represent the “end correction” as the sum:

$$\delta V_{\lambda_2\lambda_1}^{\text{end}} = \delta V_{\lambda_2\lambda_1}^Z + (\delta V_{\lambda_2\lambda_1}^{\text{end}})', \quad (27)$$

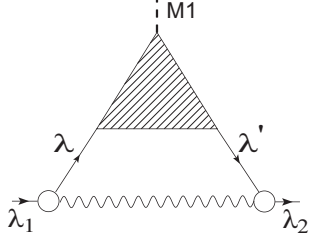


FIG. 5: The correction due to the induced interaction.

where

$$\delta V_{\lambda_2 \lambda_1}^Z = \left(\sqrt{Z_{\lambda_2} Z_{\lambda_1}} - 1 \right) V_{\lambda_2 \lambda_1}. \quad (28)$$

Eqs. (27), (28) correspond to partial summation of the diagrams of Fig. 3, and, hence, contains higher order terms in g_L^2 . To be consistent up to the order g_L^2 , the Z -factors Eq. (28) should be expanded in terms of $\partial \Sigma_{\lambda\lambda}(\varepsilon)/\partial \varepsilon$, $Z = 1 + \partial \Sigma_{\lambda\lambda}(\varepsilon)/\partial \varepsilon$, with the result

$$\delta V_{\lambda_2 \lambda_1}^Z = \frac{1}{2} \left(\left. \frac{\partial \Sigma_{\lambda_2 \lambda_2}(\varepsilon)}{\partial \varepsilon} \right|_{\varepsilon=\varepsilon_{\lambda_2}} + \left. \frac{\partial \Sigma_{\lambda_1 \lambda_1}(\varepsilon)}{\partial \varepsilon} \right|_{\varepsilon=\varepsilon_{\lambda_1}} \right) V_{\lambda_2 \lambda_1}. \quad (29)$$

This contribution is important for the conservation of the total angular momentum. This will be shown below.

As the term $\delta \Sigma^{\text{tad}}$ does not depend on the energy ε it does not contribute to Z_λ and, hence, to the main term representing the end effect which is given by Eq. (28). It may contribute to the second term of the sum of (27) which itself is negligibly small.

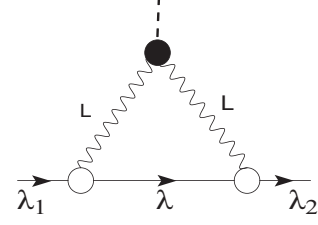
The energy derivative of the mass operator (24) is as follows:

$$\left. \frac{\partial \delta \Sigma_{\lambda\lambda}(\varepsilon)}{\partial \varepsilon} \right|_{\varepsilon=\varepsilon_\lambda} = - \sum_{\lambda' M} | \langle \lambda' | g_{LM} | \lambda \rangle |^2 \times \left[\frac{n_{\lambda'}}{(\varepsilon_\lambda + \omega_L - \varepsilon_{\lambda'})^2} + \frac{1 - n_{\lambda'}}{(\varepsilon_\lambda - \omega_L - \varepsilon_{\lambda'})^2} \right]. \quad (30)$$

Let us now go to the second line of Eq. (21) and begin with the first term containing the first variations of the wave functions. After connecting two wavy ends we obtain the “triangle” diagram (GGD) displayed in Fig. 5 which describes the effect of the induced interaction \mathcal{F}_{ind} due to exchange of the L -phonon. The explicit form of the corresponding correction to the matrix element $V_{\lambda_2 \lambda_1}$ is

$$\delta V_{\lambda_2 \lambda_1}^{GGD} = \int \frac{d\omega}{2\pi i} \sum_{\lambda' M} \langle \lambda_2 | g_{LM}^+ | \lambda' \rangle V_{\lambda' \lambda} \langle \lambda | g_{LM} | \lambda_1 \rangle \times G_\lambda(\varepsilon_{\lambda_1} - \omega) G_{\lambda'}(\varepsilon_{\lambda_2} - \omega) D_L(\omega). \quad (31)$$

After separating the angular variables and integrating over the energy, we obtain:

FIG. 6: Correction due to the direct action of the $M1$ -field to the phonon. The black blob is the magnetic moment of the phonon.

$$\delta V_{\lambda_2 \lambda_1}^{GGD} = (-1)^{j_2 - m_2} \begin{pmatrix} j_2 & 1 & j_1 \\ -m_2 & M & m_1 \end{pmatrix} \langle 2 \| \delta V^{GGD} \| 1 \rangle, \quad (32)$$

where the short notation $1 = \nu_1$ is used and the reduced matrix element is equal to

$$\langle 2 \| \delta V^{GGD} \| 1 \rangle = \sum_{34} (-1)^{L+j_4-j_3} \left\{ \begin{matrix} 1 & j_1 & j_2 \\ L & j_4 & j_3 \end{matrix} \right\} \times \langle 4 \| V \| 3 \rangle \langle 2 \| \tilde{g}_L \| 4 \rangle \langle 3 \| g_L \| 1 \rangle I_{34}(\omega_L), \quad (33)$$

$$I_{34}(\omega_L) = \frac{1}{(\varepsilon_3 - \varepsilon_4) - (\varepsilon_1 - \varepsilon_2)} \left[\frac{n_3}{\varepsilon_1 - \varepsilon_3 + \omega_L} - \frac{n_4}{\varepsilon_2 - \varepsilon_4 + \omega_L} + \frac{1 - n_3}{\varepsilon_1 - \varepsilon_3 - \omega_L} - \frac{1 - n_4}{\varepsilon_2 - \varepsilon_4 - \omega_L} \right], \quad (34)$$

where

$$\tilde{g}_L = g_L(-\omega) = g_{L0}(r; \omega) T_{LL0}(\mathbf{n}, \alpha) - g_{L1}(r; \omega) T_{LL1}(\mathbf{n}, \alpha), \quad (35)$$

Let us go to the second term in the second line of Eq. (21) with the second order variation of the effective field V . This term was considered in detail in [53]. We separate the PC correction due to the phonon contribution to the local charge e_q in the first term of Eq. (2) for the effective field. It is represented by the diagram of Fig. 6 describing the contribution of the phonon magnetic moment. It can be obtained from the first diagram of Fig. 4 by inserting the external magnetic field in the phonon line. In Fig. 6, the black blob means the phonon magnetic moment,

$$\mu_L^{\text{ph}} = g_L^{\text{ph}} L, \quad (36)$$

where g_L^{ph} is the phonon gyromagnetic ratio. In the Bohr-Mottelson model [41, 52], one has $g_{L,\text{BM}}^{\text{ph}} = Z/A$. Similar to to Eq. (31), we get

$$\delta V_{\lambda_2 \lambda_1}^{GDD} = \int \frac{d\omega}{2\pi i} \sum_{\lambda M} \langle \lambda_2 | g_{LM}^+ | \lambda \rangle \langle \lambda | g_{LM} | \lambda_1 \rangle \times G_\lambda(\varepsilon_{\lambda_1} - \omega) D_L(\omega) D_L(\omega - \omega_0). \quad (37)$$

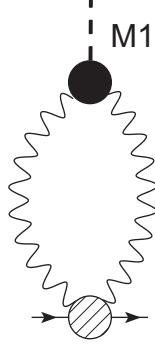


FIG. 7: The tadpole-like diagram for the contribution of the phonon magnetic moment.

Again, after separating the angular variables, we obtain for the reduced matrix element,

$$\begin{aligned} < 2 \| \delta V^{GDD} \| 1 > = \sum_3 (-1)^{L+j_1+j_3} \gamma_L \\ \times \sqrt{\frac{L(L+1)(2L+1)}{4\pi}} \left\{ \begin{matrix} j_1 & 1 & j_2 \\ L & j_3 & L \end{matrix} \right\} < 3 \| g_L \| 1 > \\ \times < 2 \| \tilde{g}_L \| 3 > \left(I_3^{(1)}(\omega_L) + I_3^{(2)}(\omega_L) \right), \end{aligned} \quad (38)$$

$$I_3^{(1)}(\omega_L) = \frac{1 - n_3}{(\varepsilon_1 - \varepsilon_3 - \omega_L)(\varepsilon_2 - \varepsilon_3 - \omega_L)} \frac{n_3}{(\varepsilon_1 - \varepsilon_3 + \omega_L)(\varepsilon_2 - \varepsilon_3 + \omega_L)}, \quad (39)$$

$$I_3^{(2)}(\omega_L) = \frac{1}{\varepsilon_1 - \varepsilon_2 - 2\omega_L} \left(\frac{n_3}{\varepsilon_2 - \varepsilon_3 + \omega_L} + \frac{1 - n_3}{\varepsilon_1 - \varepsilon_3 - \omega_L} \right) - \frac{1}{\varepsilon_1 - \varepsilon_2 + 2\omega_L} \left(\frac{1 - n_3}{\varepsilon_2 - \varepsilon_3 - \omega_L} + \frac{n_3}{\varepsilon_1 - \varepsilon_3 + \omega_L} \right). \quad (40)$$

The second integral (40) reveals a dangerous behavior at $(\omega_L - \omega_0) \rightarrow 0$. For the case of the static external field we deal, it occurs at $\omega_L \rightarrow 0$.

Analogically to producing Fig. 6 by inserting the external field to the first, pole, diagram of Fig. 4, there is the tadpole-like PC correction to the effective magnetic field which corresponds to inserting the external field to the phonon D -function in the second diagram on Fig. 4. It is displayed in Fig. 7. The dashed blob denotes the sum of all non-pole diagrams of phonon-particle scattering (the phonon-particle Compton diagrams). It contains the integral

$$I^{\text{tad}} = \int \frac{d\omega}{2\pi i} D_L(\omega) D_L(\omega - \omega_0) = \frac{4\omega_L}{\omega_L^2 - \omega_0^2}. \quad (41)$$

Its behavior at $\omega_L \rightarrow 0$ is just the same as of the integral $I_3^{(2)}$, Eq. (40). This makes it reasonable to suppose that their sum is regular at $(\omega_L - \omega_0) \rightarrow 0$.

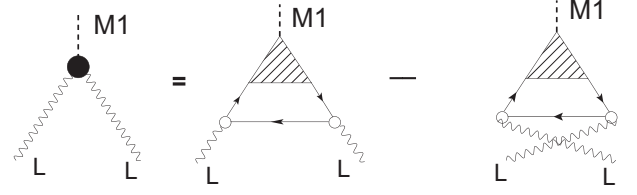


FIG. 8: Diagrams for the phonon magnetic moment in magic nuclei.

The phonon gyromagnetic ratio g_L^{ph} for magic nuclei is obtained from the diagrams shown in Fig. 8. For non-magic nuclei, the corresponding set of diagrams is much more complicated, see Ref. [33, 53] for the case of the quadrupole moment, and in this case we limit ourselves to the BM model.

Thus, the sum of the PC corrections to the effective $M1$ -field is as follows:

$$\begin{aligned} \delta V = & \delta V^Z + \delta V_{GGD} + \delta V_{GDD}^{(1)} + \delta V'_{\text{end}} \\ & + \left[\delta V_{GDD}^{(2)} + \delta V_{\text{non-pole}} \right], \end{aligned} \quad (42)$$

where $\delta V_{GDD}^{(1),(2)}$ are the terms of Eq. (37) with the integrals $I^{(1),(2)}$ and $\delta V_{\text{non-pole}}$ denotes the sum of all non-pole PC corrections to the magnetic effective field. Up to now, the method of a consistent calculation of this quantity is implemented for magic nuclei mainly [7, 42]. For non-magic nuclei, the formalism was developed in [54] but the only one realization was carried out [33]. As we shall see below, the magnitude of the first two terms of the sum (42) is, as a rule, significantly larger than that of $\delta V_{GDD}^{(1),(2)}$ terms. However, δV^Z and δV_{GGD} terms are always of the opposite sign and strongly compensate each other. Therefore, the term $\delta V_{GDD}^{(1)}$ is sometimes not negligible and should be taken into account. In the case when the external field is $V_0 = \mathbf{j}$, where $\mathbf{j} = \mathbf{l} + 1/2\boldsymbol{\sigma}$ is the total angular momentum, due to the conservation of \mathbf{j} condition, the total PC correction (42) should be zero. As we will discuss in the next section, the sum of the first four terms of (42) is equal to zero. This means that the terms $\delta V_{GDD}^{(2)}$ and $\delta V_{\text{non-pole}}$ should compensate each other. We will suppose that a similar relation is approximately valid for any $M1$ -field and will use the model where the terms in the first line of Eq. (42) are taken into account only and those on the second line are neglected. In fact, we carry out the summation of the end corrections, similar to that in Eq. (28), and the final ansatz we use is as follows:

$$\begin{aligned} \tilde{V}_{\lambda_2 \lambda_1} = & \sqrt{Z_{\lambda_2} Z_{\lambda_1}} \\ & \times \left(V + \delta V_{GGD} + \delta V_{GDD}^{(1)} + \delta V'_{\text{end}} \right)_{\lambda_2 \lambda_1}. \end{aligned} \quad (43)$$

Just as Eq. (28) vs Eqs. (22) and (25), the ansatz (43)

differs from the prescription of Eq. (42) in terms higher in g_L^2 .

In conclusion of this section, we write down the expression for the L -phonon magnetic moment μ_L in magic nuclei corresponding to Fig. 8:

$$\begin{aligned} \mu_L = & \sum_{123} (-1)^{L+1} \begin{pmatrix} 1 & L & L \\ 0 & L & -L \end{pmatrix} \begin{Bmatrix} 1 & L & L \\ j_3 & j_2 & j_1 \end{Bmatrix} \\ & \times <1 \parallel V(M1) \parallel 2> [<1 \parallel g_L \parallel 3> <3 \parallel \tilde{g}_L \parallel 2> \\ & \times I_{123}^{GGG}(\omega_L) - <1 \parallel \tilde{g}_L \parallel 3> <3 \parallel g_L \parallel 2> I_{123}^{GGG}(-\omega_L)], \quad (44) \end{aligned}$$

where

$$\begin{aligned} I_{123}^{GGG}(\omega_L) = & \frac{1}{\varepsilon_2 - \varepsilon_1} \left[\frac{n_1(1-n_2)(1-n_3) - (1-n_1)n_2n_3}{\varepsilon_1 - \varepsilon_3 - \omega_L} \right. \\ & + \frac{n_1(1-n_2)n_3 - (1-n_1)n_2(1-n_3)}{\varepsilon_2 - \varepsilon_3 - \omega_L} \Big] \\ & + \frac{n_1n_2(1-n_3) - (1-n_1)(1-n_2)n_3}{(\varepsilon_1 - \varepsilon_3 - \omega_L)(\varepsilon_2 - \varepsilon_3 - \omega_L)}. \quad (45) \end{aligned}$$

For the general case of $\omega_0 \neq 0$, $\omega'_L = \omega_L + \omega_0 \neq \omega_L$ formulae analogous to Eqs. (44) and (45) for the E2 symmetry have been obtained in Ref. [55].

B. PC corrections we omit

The diagram in Fig. 6 corresponding the variation of the local charge e_q in the effective field V is the only one example of g_L^2 PC corrections to the effective field $\delta^{(2)}V$. The main part of such corrections appears from variations of the integral term of Eq. (2). These terms were examined in detail in Refs. [43, 53, 56]. The term corresponding to the variation of the particle-hole propagator, $\delta^{(2)}A(1) = \delta^{(1)}G\delta^{(1)}G$ is displayed in Fig. 9. The wavy line for the phonon D -function, just as above, appears after connecting the phonon ends of Fig. 2. This diagram, together with that in Fig. 5, can be interpreted as the substitution of the sum $\mathcal{F}^{\text{spin}} \rightarrow \mathcal{F}^{\text{spin}} + \mathcal{F}_{\text{ind}}$ as the effective interaction in Eq. (2) with different order of these operators. Another variation of the particle-hole propagator, $\delta^{(2)}A(2) = 2\delta^{(2)}GG$, is displayed in Fig. 10. There are also more complicated diagrams for $\delta^{(2)}V$ containing mixed variations $\delta^{(1)}\mathcal{F}^{\text{spin}}\delta^{(1)}A$, see [53].

Let us discuss the reasons why we exclude these two diagrams from our model although they are of the same g_L^2 order. In fact, as it is seen from all the equations of the above subsection, g_L^2 appears always with some energy dependent denominators, and the characteristic dimensionless combination is the ratio of

$$\beta_L = \frac{(g_L)_{\lambda\lambda'}^2}{(\varepsilon_\lambda - \varepsilon_{\lambda'} \pm \omega_L)^2}. \quad (46)$$

Typical value of the matrix element $(g_L)_{\lambda\lambda'} \simeq 1$ MeV whereas the energy differences in the denominator of (46) are of the order of $\varepsilon_F/A^{1/3} \simeq 7 \div 10$ MeV. It should be reminded that we deal with “magic” sub-system of a

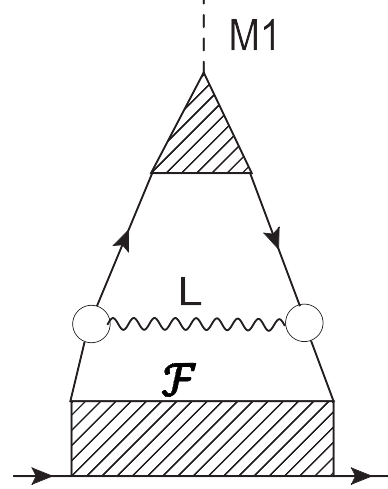


FIG. 9: The diagram alternative to the one in Fig. 5.

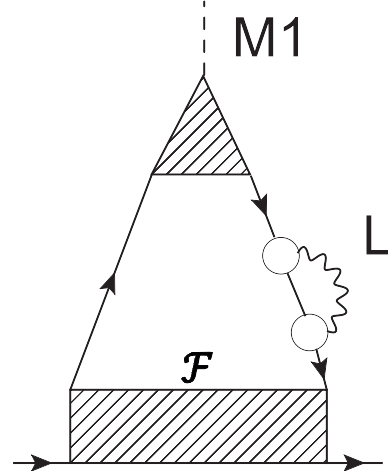


FIG. 10: A PC correction to the particle-hole propagator in Eq. (2).

semi-magic nucleus where pairing is absent. Therefore, as a rule, β_L is really a small parameter and the “ g_L^2 expansion” is justified, each separate term is small and only a large sum of such contributions can be important. Such sums do practically not depend on the nucleus under consideration and on the single-particle state of the odd nucleon. As simple estimations show, this is true for diagrams in Fig. 9 and Fig. 10. According to the strategy of our model, we must consider them as contributions to the LM amplitude $\mathcal{F}^{\text{spin}}$ and the local charge e_q and not calculate explicitly. On the other hand, as we shall see below, the PC corrections considered in the previous Subsection may depend, sometimes strongly, on

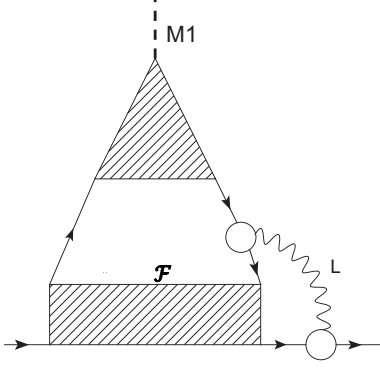


FIG. 11: An example of more complicated “mixed” diagrams corresponding to the third line of Eq. (21).

the state λ_0 of the odd nucleon with rather big contribution of a separate term with small energy denominator in β_L . Such PC corrections depend significantly on the nucleus under consideration and on the state λ_0 of the odd nucleon. They should be calculated explicitly.

Fig. 11 represents an example of the “mixed” PC corrections from the third line of Eq. (21). All arguments to exclude the two diagrams from our model remain valid for them too.

IV. PHONON MAGNETIC MOMENTS IN ^{208}Pb

In this double-magic nucleus several low-lying phonons are known with varying degree of collectivity. The lowest one 3^- possesses the highest collectivity whereas the strength of the 5^- mode is shared between two states. Before starting the study of PC effects in ^{208}Pb we analyze the accuracy of describing the phonons themselves. Their characteristics are presented in Table I. We see that the most collective 3^- level is described sufficiently well, 5_1^- and 5_2^- ones, a little worse. As to the 2_1^+ state and other states of positive parity, they are not strongly collective as there is no low-energy particle-hole configurations of positive parity except spin-orbit doublets ($h_{11/2}^{-1}h_{9/2}$) for protons and ($i_{13/2}^{-1}i_{11/2}$) for neutrons. In such a situation, ω_L values in the QRPA solution are shifted only little from the nearest particle-hole excitation energy, $\varepsilon_p(h_{9/2}) - \varepsilon_p(h_{11/2})$ or $\varepsilon_n(i_{11/2}) - \varepsilon_n(i_{13/2})$ in our case. Single-particle levels in ^{208}Pb generated with the DF3-a functional we use are displayed in Fig. 12 for neutrons and Fig. 13 for protons. Comparison is made with the experimental spectra and those obtained by us with the one of the best Skyrme functionals HFB-17 [2]. We see that our spectra reasonably agree with the data, on average, better than the HFB-17 one. However, some inaccuracy takes place for levels under consideration which is partially responsible for the shift of the 2_1^+

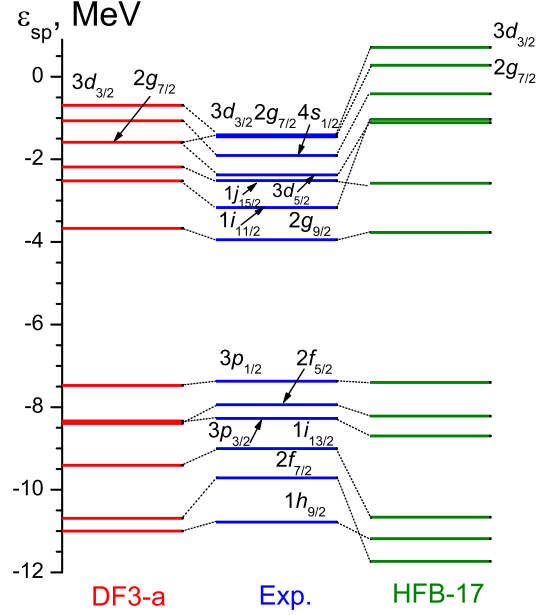


FIG. 12: Neutron single-particle levels in ^{208}Pb .

TABLE I: Characteristics of the low-lying phonons in ^{208}Pb , ω_L (MeV) and $B(EL, \text{up})(e^2\text{fm}^{2L})$.

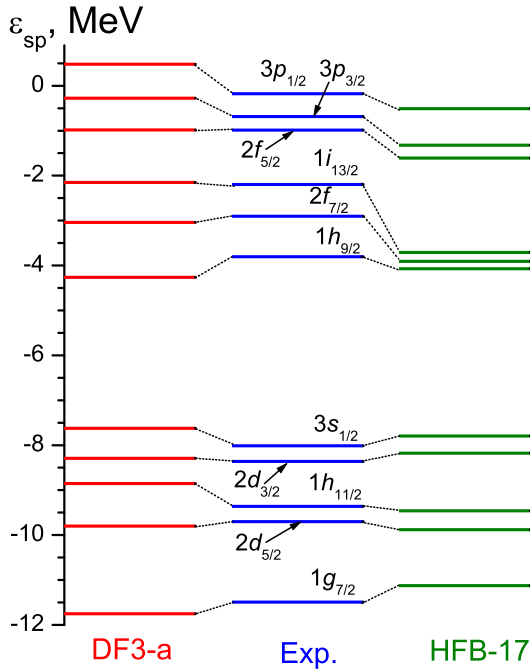
L^π	ω_L^{th}	ω_L^{exp}	$B(EL)^{\text{th}}$	$B(EL)^{\text{exp}}$
3_1^-	2.684	2.615	7.093×10^5	6.12×10^5
5_1^-	3.353	3.198	3.003×10^8	4.47×10^8
5_2^-	3.787	3.708	1.785×10^8	2.41×10^8
2_1^+	4.747	4.086	1.886×10^3	3.18×10^3
2_2^+	5.004	4.928	1.148×10^3	-
4_1^+	4.716	4.324	3.007×10^6	-
4_2^+	5.367	4.911(?)	8.462×10^6	-
6_1^+	4.735	-	6.082×10^9	-
6_2^+	5.429	-	1.744×10^{10}	-

level up to 660 keV. Another reason for this discrepancy is evidently not taking into account the spin-orbit LM amplitude in Eq. (13) for the g_L vertex. We shall see below that the PC corrections in magic nuclei originate mainly from the 3^- phonon, therefore some inaccuracy in describing higher collective states does not lead to serious errors.

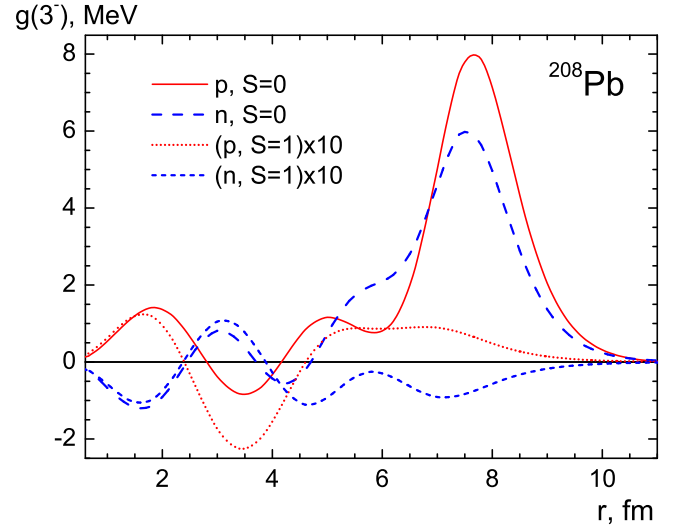
Let us now calculate magnetic moments and corresponding gyromagnetic ratios g_L^{ph} of the L -phonons in ^{208}Pb . It is given by the diagram of Fig. 8, Eq. (44). We need the g_L^{ph} values to evaluate the contribution of the phonon magnetic moment term, Fig. 6 and Eq. (38). In addition, this calculation elucidates to a large extent the structure of the phonons under consideration. The results are given in Table II. We showed separately the j - and s -components, according to Eq. (1), with obvious

TABLE II: Magnetic moments (in μ_N units) of phonons in ^{208}Pb .

L^π	$\mu_n^{(j)}$	$\mu_n^{(s)}$	μ_n	$\mu_p^{(j)}$	$\mu_p^{(s)}$	μ_p	$\mu_L^{(j)}$	$\mu_L^{(s)}$	μ_L	g_L^{ph}
3^-	-0.074	-0.039	-0.113	1.566	0.058	1.492	1.492	0.019	1.511	0.463
5_1^-	-0.027	-0.018	-0.046	4.733	0.278	5.011	4.705	0.260	4.965	0.993
5_2^-	-0.215	-0.478	-0.693	0.853	-0.123	0.730	0.638	-0.600	0.037	0.008
2_1^+	-0.027	0.000	-0.027	1.536	0.493	2.029	1.509	0.492	2.002	1.001
2_2^+	-0.027	0.004	-0.022	1.541	0.406	1.947	1.514	0.411	1.925	0.962
4_1^+	-0.009	-0.010	-0.018	4.017	0.449	4.466	4.008	0.440	4.448	1.112
4_2^+	-0.112	-0.232	-0.343	1.822	0.276	2.098	1.711	0.044	1.755	0.439
6_1^+	-0.005	-0.004	-0.009	6.172	0.294	6.466	6.167	0.290	6.457	1.076
6_2^+	-0.075	-0.147	-0.222	4.765	0.092	4.857	4.690	-0.054	4.636	0.773

FIG. 13: Proton single-particle levels in ^{208}Pb .

substitution of $\mathbf{l} = \mathbf{j} - \mathbf{s}$. The subscripts n, p refer to the neutron and proton subsystems whereas L corresponds to their sum, e.g. $\mu_L^{(j)} = \mu_n^{(j)} + \mu_p^{(j)}$. To understand better the nature of phonons we investigate it is worth comparing the g_L^{ph} values obtained with the BM model prediction $g_{L,\text{BM}}^{\text{ph}} = Z/A = 0.394$. We see that only for the 3^- and 4_2^+ -states our values are rather close to the BM one whereas in other cases there is nothing in common with these two theory predictions. Note that in the BM model the spin-component $\mu_L^{(s)}$ is absent. If we neglect in Eq. (44) the spin term of the effective field $V(M1)$ and put $\zeta_l = 0$, i.e. take $V(M1) = j$, we obtain the BM value of g_L^{ph} for all the states under considera-

FIG. 14: Components of the vertex g_L , $L^\pi = 3^-$, in ^{208}Pb .

tion. Thus, the microscopic value of the gyromagnetic ratio deviates from the classic model prediction due to the spin term and non-zero value of ζ_l .

To testify the formulas above and estimate the accuracy of the calculations, it is instructive to apply Eqs. (44), (45) to the spurious phonon $L^\pi = 1^-$, $\omega_{1^-} = 0$. In this case, the term g_{11} in the sum of Eq. (16) vanishes, whereas the term $g_{10}(\omega)$ is singular at $\omega = 0$ [7],

$$g_{10}(\omega) = \frac{1}{\sqrt{2\omega B_1}} \frac{\partial U}{\partial r}, \quad (47)$$

where $U(r)$ is the central part of the mean-field potential generated by the energy functional (9) and $B_1 = 3m/(4\pi A)$ is the BM mass coefficient [49]. Eq. (47) follows from the exact TFFS self-consistency relation [9] with some simplifications and neglecting the spin-orbit terms. The singularity in all the above expressions containing g_1^2 is compensated as the corresponding integrals of the Green functions are proportional to ω . This ap-

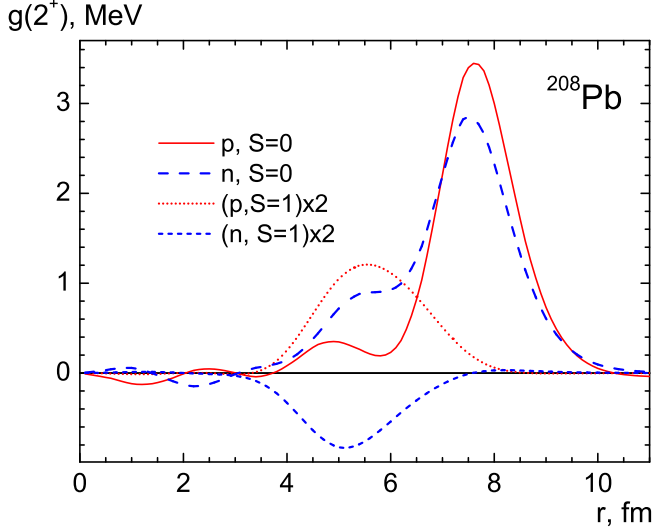


FIG. 15: Components of the vertex g_L , $L^\pi = 5_1^-$, in ^{208}Pb .

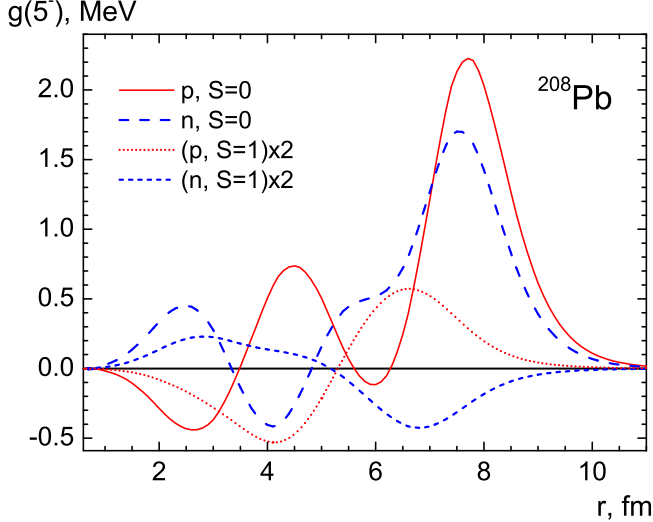


FIG. 16: Components of the vertex g_L , $L^\pi = 2_1^+$, in ^{208}Pb .

proximation for g_1 violates a little the normalization relation (14) leading to the value -1.074 instead of -1. If we correct normalization, we obtain for the magnetic moment of the spurious 1^- -phonon we obtain $\mu(1^-) = 0.403$ in very good agreement with the BM gyromagnetic ratio 0.394. This calculation confirms the self-consistency of the scheme developed above.

In our calculations, the spin component is negligible for the 3^- -state only. It confirms that this state, indeed, is most similar to the BM surface vibrations. The phonon

creation amplitudes g_L are displayed in Figs. 11-13 for the states 3^- , 5_1^- and 2_1^+ , respectively. We see that all of them contain the BM-like ($\propto \partial U/\partial r$) surface maxima of the spin-zero components which are significantly larger than components with $S = 1$. However, for 5_1^- and 2_1^+ states they are not negligible. Moreover, they possess maxima at $r \simeq 6$ fm where the wave functions of the single-particle states in vicinity of Fermi level have their maxima too. This is true for couples of the wave functions ($\phi_\lambda \phi_{\lambda'}$) which correspond to the term with a small energy denominator in Eq. (45) which always exists for the phonon states under discussion. At the same time the maxima of the main, $S = 0$, components are shifted to the right at $\simeq 1 \div 2$ fm due to the coherent contribution of a lot of single-particle states distant from Fermi surface. However, in this region the wave functions under discussion began vanish. As the result, for these states the contribution of the $S = 1$ to the phonon magnetic moment is often rather big.

V. J-CONSERVATION CONDITION

As the total angular momentum $\mathbf{j} = \mathbf{l} + 1/2\boldsymbol{\sigma}$ is the integral of motion, the identity

$$V(\mathbf{j}) = \mathbf{j} \quad (48)$$

should be fulfilled. Within the standard TFFS, it leads to relations for the local charges $e_q^{n,p}$ [8]. Obviously, when the PC corrections are included, the sum of all of them discussed above should vanish in the case of $V_0 = \mathbf{j}$. As it was mentioned in Sect. 3, the sum of the first four terms of (42) is equal to zero for any value of L . This can be shown analytically and by numerical calculations as well.

This means that the identity

$$\delta V_{\text{non-pole}}(\mathbf{j}) = -\delta V_{GDD}^{(2)}(\mathbf{j}) \quad (49)$$

should be fulfilled to guarantee the identity (48). We suppose that the similar relation,

$$\delta V_{\text{non-pole}}(M1) = -\delta V_{GDD}^{(2)}(M1), \quad (50)$$

is valid for the complete $M1$ -field. This relation is the main ingredient of the model we use.

It is worth noting that the ansatz (43) violates the \mathbf{j} -conservation law as it takes into account higher order terms in g_L^2 in a non-consistent way. However, this violation turned out to be rather small.

VI. MAGNETIC MOMENTS OF THE ODD NEIGHBORS OF ^{208}Pb

As it was mentioned above the first two terms of Eq. (42) dominate. Let us begin from the “end correction” which is simpler for the analysis. In Table III we show contributions of three phonons to the Z -factors

TABLE III: Contributions of different low-lying phonons to the Z -factors of single-particle states in ^{208}Pb .

λ	$Z(3_1^-)$	$Z(5_1^-)$	$Z(2_1^+)$	Z'	Z_{tot}
$3d_{5/2}^n$	0.963	0.989	0.967	0.944	0.869
$1j_{15/2}^n$	0.657	0.985	0.989	0.974	0.623
$1i_{11/2}^n$	0.974	0.998	0.990	0.981	0.944
$2g_{9/2}^n$	0.918	0.995	0.989	0.975	0.881
$3p_{1/2}^n$	0.963	0.995	0.986	0.979	0.925
$3p_{3/2}^n$	0.960	0.992	0.984	0.971	0.910
$2f_{5/2}^n$	0.964	0.997	0.985	0.974	0.922
$1i_{13/2}^n$	0.943	0.990	0.990	0.979	0.904
$2f_{5/2}^p$	0.953	0.995	0.941	0.907	0.810
$1i_{13/2}^p$	0.747	0.992	0.993	0.975	0.718
$2f_{7/2}^p$	0.898	0.996	0.991	0.971	0.861
$1h_{9/2}^p$	0.978	0.999	0.996	0.987	0.960
$3s_{1/2}^p$	0.959	0.996	0.992	0.979	0.928
$2d_{3/2}^p$	0.964	0.998	0.992	0.982	0.937
$1h_{11/2}^p$	0.951	0.996	0.995	0.982	0.926
$2d_{5/2}^p$	0.758	0.996	0.986	0.968	0.721

of different single-particle states in the odd neighbors of ^{208}Pb , i.e. in $^{207,209}\text{Pb}$ isotopes for neutrons and ^{207}Tl , ^{209}Bi nuclei for protons. Here, we used the notation $Z_{\text{tot}} = \prod_{i=1}^9 Z_i$ and $Z' = Z_3 \prod_{i=5}^9 Z_i$, where the index i numerates all the collective states listed in Table I. Thus, the states 3_1^- , 5_1^- and 2_1^+ are excluded in Z' .

As it was stated in the Introduction, the contribution of the 3^- state to the PC corrections dominates in magic nuclei due to its strong collectivity. Table III confirms this statement on average, although often the the sum of the contributions of all other phonons to the difference of $(1 - Z_\lambda)$ is comparable with the one of the 3^- phonon alone. From the other phonons, the 2_1^+ phonon contributes most to the Z -factor although it is less collective than 5_1^- , 5_2^- phonons. The reason becomes clear if one looks to Eq. (30) which determines the phonon contribution to the difference of $(1 - Z_\lambda)$, see also Eq. (46) which gives an estimate of a separate contribution to different PC correction. It is obvious that the situation is on average more preferable for phonons of positive parity. Indeed, in this case the states λ, λ' in (46) are of the same parity and it is easier to find those single-particle states with a “small denominator”. That is why there are two cases, the $3d_{5/2}^n$ and $2f_{5/2}^p$ states, where the contribution of the 2_1^+ phonon to the difference of $(1 - Z_\lambda)$ is comparable with the one of the 3^- phonon, although the matrix elements of g_2 are typically three times smaller than those of g_3 . Typical value of the Z -factor in ^{208}Pb is $Z_{\text{tot}} = 0.8 \div 0.9$. In this case, the perturbation theory in g^2 should work well. However, there are one neutron state, $1j_{15/2}^n$, and two proton ones, $1j_{13/2}^p$ and $2d_{5/2}^p$, for which we have $Z_{\text{tot}} = 0.7 \div 0.6$ and application of the perturbation theory is questionable.

Table IV contains various PC corrections to magnetic

moments of odd neighbors of ^{208}Pb . In agreement with the above ansatz, the total value of $\delta\mu$ given in the last column is the sum of the terms in the first line of Eq. (42). The term $\delta\mu_{GDD}^{(2)}$ is presented just for information. In the upper part of the table five cases are presented for which experimental data exist. We see that for all of them the PC correction to μ value is negligible. The reason is the strong cancelation of the first two corrections, $\delta\mu^Z$ and $\delta\mu_{GDD}$. The term $\delta\mu_{GDD}^{(1)}$ is usually significantly smaller than these two main ones. The term $\delta\mu'_{\text{end}}$ is defined in accordance with Eq. (27). This correction is always negligible and is included just for completeness.

In the two bottom lines of Table IV we presented two examples of strong PC corrections for two states which magnetic moments are not known. In both cases, the PC correction to the Z -factor is rather big, see Table III, because of the existence of a term with small energy denominator, see Eq. (46), for the 3^- -phonon. Due to the same reason, the term $\delta\mu_{GDD}^{(1)}$ is also rather big. In the case of the $1j_{15/2}^n$ state, $\delta\mu^Z$ and $\delta\mu_{GDD}$ terms again cancel each other, but the $\delta\mu_{GDD}^{(1)}$ term is comparable with the first two terms and leads to a big total correction. In the $1i_{13/2}^p$ case, the cancelation is not so strong as usual, but the $\delta\mu_{GDD}^{(1)}$ term is again important.

Table V contains the final results for magnetic moments,

$$\mu_{\text{th}} = \mu_0 + \delta\mu, \quad (51)$$

where the first term is the TFFS prediction for the magnetic moment, i.e. the solution of Eq. (2), and $\delta\mu$ is the sum of all the PC corrections considered above. We see that they can not help in solving the long-standing problem of the theoretical description of the ground state magnetic moment of the ^{209}Bi nucleus. Evidently, in this case the usual TFFS form (6) for the spin-dependent LM amplitudes is not sufficient and the spin-orbit terms and tensor ones in cross channel should be included. This is rather difficult in the coordinate space method we use for solving Eq. (2). The direct solution in the λ -representation in a large basis would be more adequate in this case. Importance of the spin-orbit force for this problem was found in Ref. [57].

In conclusion of this Section, we repeat that our model for PC contributions to magnetic moments of odd neighbors of ^{208}Pb leads to very small corrections. A similar result was obtained previously by Tselyaev [43] who considered mainly diagrams we omit, displayed in Fig. 9 and Fig. 10. The reason was in strong cancelation of these diagrams similar to cancelation of the diagrams in Fig. 3 and Fig. 5 within our model.

VII. MAGNETIC MOMENTS OF SEMI-MAGIC NUCLEI

Let us go to semi-magic nuclei. As it was mentioned in the Introduction, we deal with such odd nuclei where

TABLE IV: PC contributions to the magnetic moments (in μ_N) of odd neighbors of ^{208}Pb . The notation is explained in the text.

nucleus	λ	μ_0	L^π	$\delta\mu^Z$	$\delta\mu_{GGD}$	$\delta\mu_{GGD}^{(1)}$	$(\delta\mu_{GGD}^{(2)})$	$\delta\mu'_{\text{end}}$	$\delta\mu_{\text{PC}}$
^{207}Pb	$3p_{1/2}^{-n}$	0.474	3_1^-	-0.018	0.015	-0.2E-3	0.018	0.5E-3	-0.003
			all	-0.037	0.030	0.006	0.031	0.002	0.001
^{207}Pb	$2f_{5/2}^{-n}$	0.720	3_1^-	-0.027	0.019	-0.001	0.071	-0.002	-0.011
			all	-0.058	0.046	0.050	0.140	-0.002	0.036
^{209}Pb	$2g_{9/2}^n$	-1.337	3_1^-	0.120	-0.111	-0.051	0.166	0.007	-0.035
			all	0.174	-0.154	-0.013	0.157	0.008	0.015
^{207}Tl	$3s_{1/2}^{-p}$	1.857	3_1^-	-0.082	0.089	-0.004	0.005	-0.004	-0.001
			all	-0.137	0.130	-0.005	0.001	0.035	0.023
^{209}Bi	$1h_{9/2}^p$	3.691	3_1^-	-0.083	0.051	0.014	0.048	0.002	-0.015
			all	-0.146	0.096	0.033	0.041	0.002	-0.015
^{209}Pb	$1j_{15/2}^n$	-1.315	3_1^-	0.688	-0.679	0.696	-0.237	-0.001	0.703
			all	0.754	-0.738	0.780	-0.249	-0.001	0.794
^{209}Bi	$1i_{13/2}^p$	8.071	3_1^-	-2.730	1.530	0.413	-0.162	0.3E-3	-0.785
			all	-3.020	1.730	0.460	-0.178	0.001	-0.824

TABLE V: Magnetic moments (in μ_N units) of the odd neighbors of ^{208}Pb .

nucleus	λ	μ_0	$\delta\mu$	μ_{th}	μ_{exp}
^{207}Pb	$3p_{1/2}^{-n}$	0.474	0.001	0.475	0.592585(9)
^{207}Pb	$2f_{5/2}^{-n}$	0.720	0.036	0.756	0.80(3)
^{209}Pb	$2g_{9/2}^n$	-1.337	0.015	-1.322	-1.4735(16)
^{209}Pb	$1j_{15/2}^n$	-1.315	0.794	-0.521	-
^{207}Tl	$3s_{1/2}^{-p}$	1.857	0.023	1.880	1.876(5)
^{209}Bi	$1h_{9/2}^p$	3.691	-0.015	3.676	4.1106(2)
^{209}Bi	$1i_{13/2}^p$	8.071	-0.824	7.247	-

the odd nucleon belongs to the non-superfluid subsystem. Otherwise, all equations of Sect. 3 should be generalized by including the superfluidity. In particular, we consider the odd-proton neighbors of the even lead nuclei, i.e. Tl and Bi isotopes, and the same for the tin-core region, where we analyze In and Sb isotopes. However, the neutron sub-system which is now superfluid and we have to apply the vector notation of Eq. (15) using the initial notation $g_L^{(0)}$ for the normal component of \hat{g}_L and $g_L^{(1,2)}$ for the anomalous ones. All the equations of Section 3 remain valid with the only exception of Eqs. (44), (45) corresponding to Fig. 8, for the phonon magnetic moment or the gyromagnetic ration g_L^{ph} . Indeed, now the neutron triangle should be included also, with taking into account the superfluidity effects. Therefore we use the BM model prediction for g_L^{ph} in this Section. This is justified as far as we consider only such phonons which are very collective.

In all even-even spherical non-magic nuclei there exists

TABLE VI: Characteristics of the low-lying 2_1^+ -phonons in even Pb isotopes, ω_2 (MeV) and $B(E2, \text{up}) \times 10^4 (\text{e}^2 \text{fm}^4)$.

A	ω_2^{th}	ω_2^{exp}	$B(E2)^{\text{th}}$	$B(E2)^{\text{exp}}$
188	1.028	0.723	0.551	-
190	0.930	0.733	0.617	-
192	0.849	0.853	0.634	-
194	0.792	0.965	0.646	-
196	0.764	1.049	0.627	-
198	0.762	1.063	0.624	-
200	0.789	1.026	0.479	-
202	0.823	0.960	0.373	-
204	0.882	0.899	0.250	0.162 (0.004)
206	0.945	0.803	0.130	0.100 (0.002)
208	4.747	4.086	0.189	0.30 (0.03)
210	1.346	0.799	0.036	0.051 (0.015)
212	1.443	0.804	0.131	-
214	1.125	0.836	0.161	-

a very collective low-lying 2_1^+ -state with an excitation energy $\omega_{2+} \simeq 1$ MeV. In fact, it is the only state which should be taken into account for the PC corrections to magnetic moments. For the odd-proton neighbors of nuclei $^{200-206}\text{Pb}$ we included also the 3_1^- -state, the next in the range of collectivity, and found that it gives only several % of the main PC correction of the 2_1^+ -state. Therefore in other cases we limit ourselves with this PC correction only. In Table IV we present excitation energies and $B(E2)$ values of the even Pb isotopes.

These results were reported previously in [15]. Experimental data on $B(E2)$ values are not complete whereas the ω_{2+} value is known for all isotopes in the chain we consider. As the analysis in the previous Section showed

TABLE VII: Z -factor values of two proton levels close to the Fermi surface due to the 2_1^+ and 3_1^- -phonons in the lead chain.

A	$Z(3s_{1/2})[2^+]$	$Z(3s_{1/2})[3^-]$	$Z(1h_{9/2})[2^+]$	$Z(1h_{9/2})[3^-]$
188	0.830	-	0.659	-
190	0.822	-	0.614	-
192	0.834	-	0.605	-
194	0.719	-	0.542	-
196	0.824	-	0.547	-
198	0.810	-	0.526	-
200	0.755	0.966	0.619	0.980
202	0.743	0.967	0.628	0.981
204	0.856	0.968	0.786	0.982
206	0.915	0.965	0.880	0.981

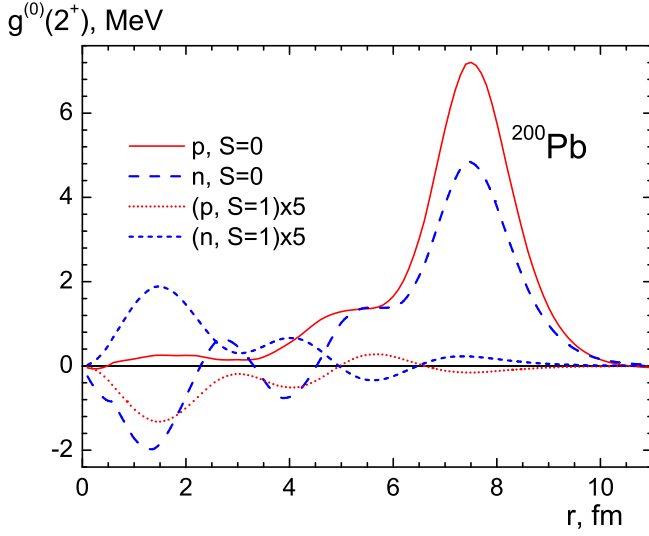


FIG. 17: Components of the normal amplitude $g_2^{(0)}$ in ^{200}Pb .

the latter is of primary importance for calculating the PC corrections. We see that the excitation energies on average are in reasonable agreement with the data. However, the theory does not reproduce the experimental trend. Specifically, if we exclude the magic ^{208}Pb nucleus, the experimental ω_{2^+} values have a maximum, $\simeq 1$ MeV, in the middle of the chain, $A \simeq 200$, and decrease to $\simeq 0.7 \div 0.8$ MeV at both ends. The theoretical predictions have opposite behavior. They show in the middle a minimum, $\simeq 0.8$ MeV, and increase up to $\simeq 1$ MeV in the left end and up to $\simeq 1.4$ MeV in the right one. Therefore we may expect that our predictions for $\delta\mu_{\text{PC}}$ values will be too high in the middle of the chain and too low in the both ends. However, as the estimation (46) shows, the position of single-particle levels in the Fermi surface vicinity are often as important as the ω_L value. In the very right end of the chain the difference of $\omega_2^{\text{th}} - \omega_2^{\text{exp}}$ reaches so large value as 0.6 MeV. In view of such de-

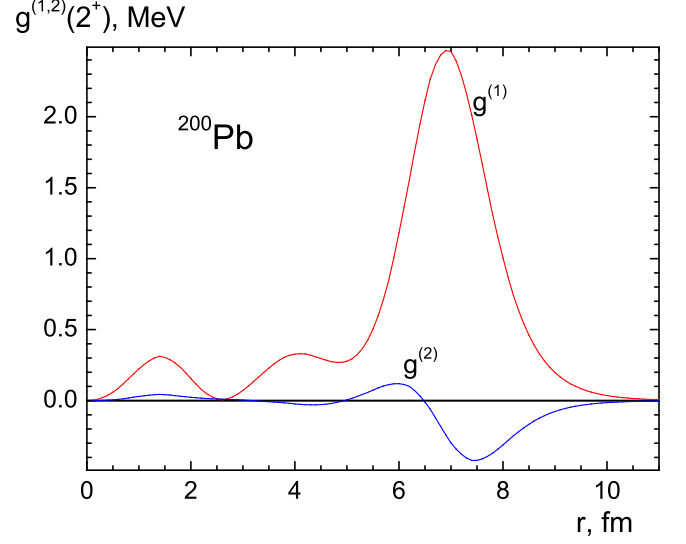


FIG. 18: Components of the neutron anomalous amplitudes $g_2^{(1)}$ and $g_2^{(2)}$ in ^{200}Pb .

ficiency, we may wait most errors of our predictions for PC corrections in this part of the chain.

In Fig. 17 we display the components of the normal amplitude $g_L^{(0)}$ in ^{200}Pb which is in the middle of the lead chain. For graphical convenience the spin-one components are multiplied by the factor of 5. Remind that, in fact, we deal with the proton vertices only. We see that, just as for the 3^- -state in ^{208}Pb , the spin-one component is negligible and can be neglected. For completeness we present also in Fig. 18 the neutron anomalous amplitudes $g_L^{(1)}$, $g_L^{(2)}$, spin-zero components only. We see that the first of them is rather big, comparable to the normal vertex $g_L^{(0)}$. Note that all the components of the vector \hat{g}_L are normalized with the same normalization condition (14) and can be compared directly.

To estimate the scale of the PC corrections, it is instructive to analyze the Z -factors of the states we consider. We deal with the odd Tl isotopes with $3s_{1/2}$ state for the odd proton and the odd Bi isotopes with $1g_{9/2}$ state for the odd proton. Corresponding values of the Z -factors induced by the 2_1^+ -state are given in Table VII. For lead cores $A = 200 \div 206$ we showed also the Z -factor induced by the 3_1^- -state. We see that it is rather close to unit, so that $Z_{\text{tot}} = Z(2^+)Z(3^-) \simeq Z(2^+)$. This is a signal that all the PC corrections due to the 3_1^- -state are now very small and those from the 2_1^+ -state could be taken into account only.

We see that for the major part of the lead isotopes the Z -factors deviate from unit significantly, $Z \simeq 0.5 \div 0.6$. This occurs because in the sum of Eq. (30) which determines the Z -factor there is one or two “dangerous” terms with small energy denominators for which the perturba-

tion parameter (46) is not small. In such a situation, the perturbational in g_L^2 theory becomes doubtful and one has to consider higher order corrections. There is a simple way to take into account some of them. Let us separate the PC correction to the effective field, the first line of Eq. (42), into two components,

$$\delta V = \delta V^Z + \delta V', \quad (52)$$

and the PC correction to the magnetic moment,

$$\delta\mu = \delta\mu^Z + \delta\mu'. \quad (53)$$

Instead of the direct perturbation formula for the magnetic moment (51) we will use also the following ansatz:

$$\tilde{\mu}_{\text{th}} = Z_\lambda(\mu_0 + \delta\mu'). \quad (54)$$

The physical meaning of this recipe is very simple. It corresponds to introducing the “end correction” similar to that of Fig. 3 not only to the effective field $V(M1)$ itself, but also to triangle diagrams of Fig. 5 and Fig. 6 describing other types of the PC corrections. Of course, this is just an intuitive ansatz and a consistent way to consider the dangerous terms is necessary. Up to now it is not developed and we present in Fig. 19 both predictions for Tl isotopes of Eq. (51) corresponding to the g_L^2 -approximation and of the ansatz (54) where also some higher in g_L^2 terms are considered. In this case, the absolute value of the PC correction of Eq. (54) is reduced, although the difference between these two results is rather small.

We see that for all isotopes of this chain except ^{207}Tl , i.e. all non-magic ones, the sign of the PC correction is negative which always helps to reproduce the data. The experimental μ value undergoes a sharp jump from ^{207}Tl to ^{205}Tl remaining almost constant for lighter isotopes. The PC correction describes such a behavior only qualitatively. Its absolute value grows smoothly till $^{199,201}\text{Tl}$ and becomes again rather small for lighter isotopes. Table VIII shows separate components of $\delta\mu$, with the same notation as in Table V. Again, as it took place for the odd neighbors of the magic ^{208}Pb , the resulting $\delta\mu$ value is much smaller than the terms $\delta\mu^Z$ and $\delta\mu_{GGD}$ separately which have opposite signs and compensate each other strongly. Other components of $\delta\mu$ again are less important. However, the sign of the $\delta\mu_{GGD}^{(1)}$ term is the same as of $\delta\mu_{GGD}$ and “helps” to diminish the total $\delta\mu$ value.

Similar results for Bi isotopes are displayed in Fig. 20 and separate terms of $\delta\mu$ are presented in Table IX. Now the cancelation of different PC corrections is even stronger than for the Tl isotopes, and the $|\delta\mu|$ value is usually 10 or 15 times less than $|\delta\mu^Z|$. Contrary to the Tl case, now the sign of the PC correction looks incorrect. However, the main reason for the contradiction between the theory and experiment is evidently incorrect value of μ_0 . Indeed, in ^{209}Bi where the PC correction is negligible, see Section 5, we have $\mu_{\text{exp}} - \mu_0 \simeq 0.5 \mu_N$. As it

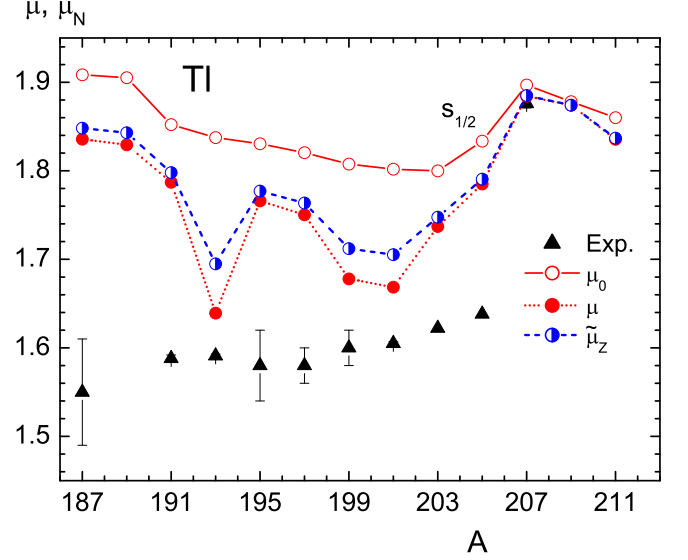


FIG. 19: Magnetic moments of Tl isotopes.

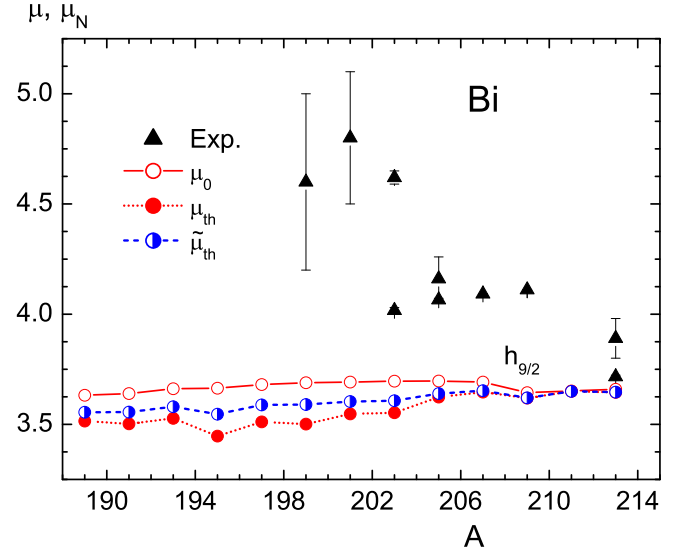


FIG. 20: (Magnetic moments of Bi isotopes.

was discussed above, the main reason for this deviation is supposedly absence of the spin-orbit and additional tensor terms in the spin-dependent LM interaction (6). In any case, the final conclusion about the sign of the PC corrections could be made only after solving the problem of ^{209}Bi .

Let us go to the tin region. Again we consider the proton-odd neighbors of even Sn isotopes, the odd In and Sb isotopes, with non-superfluid proton sub-systems.

TABLE VIII: PC contributions to the magnetic moments (in μ_N) of odd Tl isotopes, $\lambda_0 = 3s_{1/2}^-$. The notation is explained in the text nearby Table IV.

A	μ_{exp}	μ_0	L^π	$\delta\mu^Z$	$\delta\mu_{GDD}$	$\delta\mu_{GDD}^{(1)}$	$(\delta\mu_{GDD}^{(2)})$	$\delta\mu'_{\text{end}}$	$\delta\mu_{\text{tot}}$	μ_{th}	$\tilde{\mu}_{\text{th}}$
207	+1.876(5)	1.857	all	-0.137	0.130	-0.005	0.001	0.035	0.023	1.884	1.885
205	+1.63821461(12)	1.834	$2^+ + 3^-$	-0.236	0.175	0.014	0.022	-0.003	-0.048	1.785	1.791
203	+1.62225787(12)	1.800	$2^+ + 3^-$	-0.363	0.281	0.022	0.027	-0.003	-0.063	1.737	1.748
201	+1.605(2)	1.802	$2^+ + 3^-$	-0.684	0.505	0.049	0.057	-0.001	-0.133	1.669	1.705
199	+1.60(2)	1.808	$2^+ + 3^-$	-0.649	0.475	0.047	0.057	-0.003	-0.130	1.678	1.712
197	+1.58(2)	1.820	2^+	-0.426	0.332	0.025	0.036	0.0	-0.070	1.750	1.764
195	+1.58(4)	1.831	2^+	-0.390	0.303	0.023	0.034	0.0	-0.065	1.766	1.777
193	+1.5912(22)	1.838	2^+	-0.717	0.442	0.076	0.089	0.001	-0.198	1.639	1.695
191	1.588(4)	1.852	2^+	-0.370	0.281	0.023	0.032	0.0	-0.065	1.787	1.798
189	-	1.905	2^+	-0.413	0.310	0.027	0.034	0.0	-0.076	1.829	1.843
187	-	1.908	2^+	-0.391	0.292	0.026	0.031	0.0	-0.073	1.836	1.848

TABLE IX: PC contributions to the magnetic moments (in μ_N) of odd Bi isotopes, $\lambda_0 = 1g_{9/2}^-$. The notation is explained in the text nearby Table IV.

A	μ_{exp}	μ_0	L^π	$\delta\mu^Z$	$\delta\mu_{GDD}$	$\delta\mu_{GDD}^{(1)}$	$(\delta\mu_{GDD}^{(2)})$	$\delta\mu'_{\text{end}}$	$\delta\mu_{\text{tot}}$	μ_{th}	$\tilde{\mu}_{\text{th}}$
213	+3.717(13)	3.659	2^+	-0.196	0.170	0.013	-0.013	-0.001	-0.014	3.645	3.646
211	3.5(3)	3.651	2^+	-0.029	0.026	0.002	-0.001	0.0	-0.002	3.650	3.650
209	+4.1106(2)	3.691	all	-0.146	0.096	0.033	0.041	0.002	-0.015	3.619	3.620
207	+4.0915(9)	3.692	$2^+ + 3^-$	-0.575	0.485	0.043	0.001	0.002	-0.045	3.647	3.653
205	+4.065(7)	3.696	$2^+ + 3^-$	-1.072	0.922	0.074	-0.032	0.003	-0.073	3.624	3.640
203	+4.017(13)	3.696	$2^+ + 3^-$	-2.263	1.965	0.151	-0.109	0.004	-0.143	3.553	3.607
201	4.8(3)	3.692	$2^+ + 3^-$	-2.344	2.037	0.158	-0.109	0.004	-0.145	3.547	3.604
199	+4.6(4)	3.689	2^+	-3.330	2.925	0.215	-0.218	0.002	-0.188	3.501	3.590

The calculation scheme is the same as for the Tl and Bi chains, in particular, we use the BM values for the phonon gyromagnetic ratio. On the base of experience of calculations in the lead region, in all superfluid tin nuclei we consider the 2_1^+ states only except for the magic ^{100}Sn and ^{132}Sn where we include also the 3_1^- state. In Table X the characteristics of the 2_1^+ states, excitation energies and $B(E2)$ values, are given. They, just as those for the lead isotopes, were reported in [15]. As it is follows from the above analysis, the excitation energy ω_2 is of primary importance for accuracy of calculations of the PC corrections. We see that, with several exceptions, ω_2 value is reproduced with accuracy $100 \div 200$ keV i.e. sufficiently well. The $B(E2)$ values characterize the “strength” of the phonon coupling amplitudes g_L , and they are also reproduced reasonably.

In Table XI, the Z -factor values are shown for three states λ_0 nearby the Fermi surface, just the same which are involved in In and Sb nuclei we analyze. We see that there are several cases where the Z -factors are very small, $1 - Z \ll 1$. This is a signal that there is a catastrophic term with a small denominator in Eq. (46). E.g., in the ^{110}Sn case, for $Z(1g_{7/2})$ we have $\varepsilon_{1g_{7/2}} - \varepsilon_{2d_{5/2}} - \omega_L = 0.08$ MeV. It's clear that in such a situation the perturbation expansion in g_L^2 , in fact, in β_L of Eq. (46) is absolutely non-realistic, and an exact account of the

TABLE X: Characteristics of the low-lying 2_1^+ -phonons in even Sn isotopes, ω_2 (MeV) and $B(E2, \text{up}) \times 10^4 (\text{e}^2 \text{fm}^4)$.

A	ω_2^{th}	ω_2^{exp}	$B(E2)^{\text{th}}$	$B(E2)^{\text{exp}}$
102	1.453	1.472	0.065	-
104	1.388	1.260	0.107	-
106	1.316	1.207	0.142	0.195 (0.039)
108	1.231	1.206	0.155	0.222 (0.019)
110	1.162	1.212	0.188	0.220 (0.022)
112	1.130	1.257	0.197	0.240 (0.014)
114	1.156	1.300	0.193	0.24 (0.05)
116	1.186	1.294	0.182	0.209 (0.006)
118	1.217	1.230	0.172	0.209 (0.008)
120	1.240	1.171	0.152	0.202 (0.004)
122	1.290	1.141	0.158	0.192 (0.004)
124	1.350	1.132	0.147	0.166 (0.004)
126	1.405	1.141	0.120	0.10 (0.03)
128	1.485	1.169	0.094	0.073 (0.006)
130	1.610	1.221	0.055	0.023 (0.005)
132	4.327	4.041	0.104	0.11 (0.03)
134	1.142	0.725	0.033	0.029 (0.005)

dangerous terms is necessary. Fortunately, the nuclei for which experimental data exist are out of this catastrophic region.

TABLE XI: Z -factor values of proton levels close to the Fermi surface induced by the low-lying phonons in the tin chain.

A	$Z(1g_{9/2})$	$Z(2d_{5/2})$	$Z(1g_{7/2})$
100	0.939	0.910	0.933
102	0.818	0.783	0.524
104	0.716	0.673	0.344
106	0.634	0.592	0.238
108	0.584	0.549	0.158
110	0.509	0.481	0.103
112	0.482	0.464	0.458
114	0.510	0.484	0.238
116	0.609	0.582	0.414
118	0.578	0.547	0.454
120	0.614	0.591	0.607
122	0.634	0.605	0.591
124	0.674	0.648	0.651
126	0.734	0.712	0.725
128	0.800	0.780	0.798
130	0.914	0.878	0.836
132	0.962	0.923	0.968

Just as for the lead chain above, we display in Fig. 21 the components of the normal amplitude $g_L^{(0)}$ in the ^{118}Sn nuclei which is chosen as a representative of the tin chain. For graphical convenience the spin-one components are multiplied by the factor of 5. As before, we deal with the proton vertices only. We see that again this mode is a typical surface vibration, the spin-one component is very small and can be neglected. For completeness we present again in Fig. 22 the neutron spin-zero components of the anomalous amplitudes $g_L^{(1)}$ $g_L^{(2)}$. We see that both of them are rather large and have the surface maxima of opposite sign. In the result, the amplitude $g_L^{\text{an},+} = g_L^{(1)} + g_L^{(2)}$ is very small whereas the amplitude $g_L^{\text{an},-} = g_L^{(1)} - g_L^{(2)}$ is comparable with the normal amplitude $g_L^{(0)}$. This point is out of the scope of this article but it worth to note that the latter combination determines the collective phenomena in superfluid sub-system [1, 8].

Let us go to PC corrections to magnetic moments and begin with odd In nuclei. In this chain, there are 13 isotopes with known experimental values of magnetic moments of the ground state $9/2^+$ corresponding to the $g_{9/2}^{-p}$ hole in the corresponding even core of Sn. The theoretical predictions for the magnetic moments are displayed in Fig. 23 whereas separate components of the PC correction are given in Table XII. We see that the TFFS prediction without PC corrections overestimates the experimental value by $\simeq 0.4 \mu_N$. The value of $\delta\mu_{\text{tot}}$, column 10 of Table XII, is always negative and in general large enough to compensate this excess. In $^{109-113}\text{In}$ isotopes the PC correction is even too large. This correlates with small values of the $Z \simeq 0.5$ which corresponds to $\partial\Sigma/\partial\varepsilon \simeq -1$. It is worth noting that even the biggest total PC correction $\delta\mu_{\text{tot}} \simeq -0.6 \mu_N$ is the result of an almost exact compensation of the two ten times bigger corrections $\delta\mu^Z$ and $\delta\mu_{GGD}$. Therefore any additional

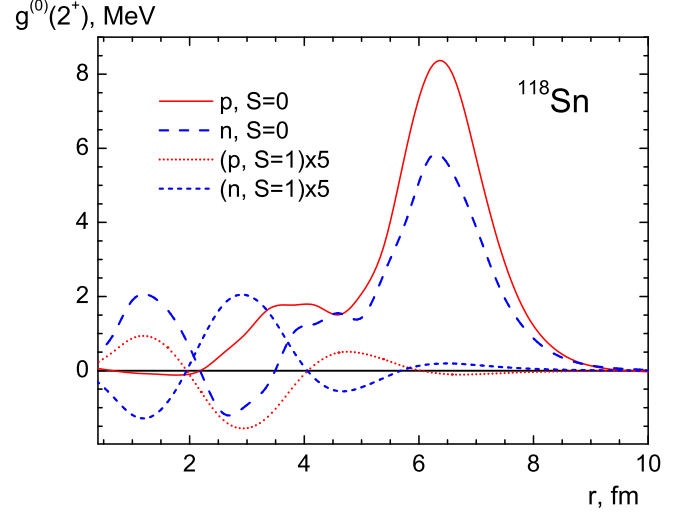


FIG. 21: Components of the normal amplitude $g_2^{(0)}$ in ^{118}Sn .

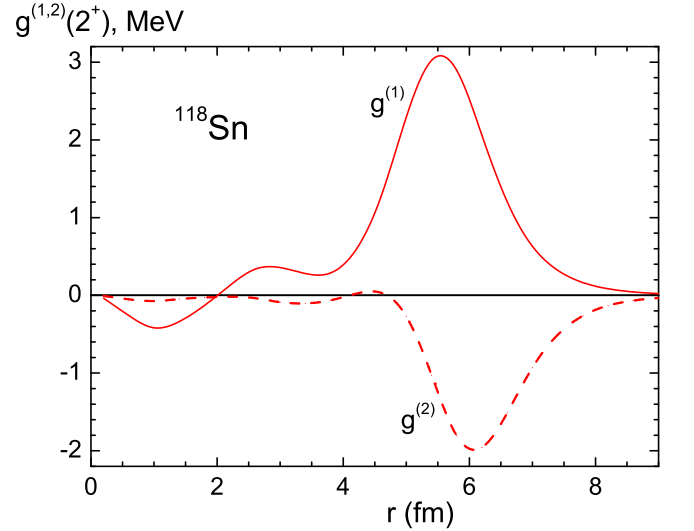


FIG. 22: Components of the neutron anomalous amplitudes $g_2^{(1)}$ and $g_2^{(2)}$ in ^{118}Sn .

term can change the results significantly. The PC correction is reduced in this case by almost a factor two if we use the ansatz (54), $\mu_{\text{th}} \rightarrow \tilde{\mu}_{\text{th}}$. Remind that it is an approximate way to take into account some higher order terms in g_L^2 corresponding to partial summation of the pole end diagrams. As it was discussed above, so large PC effect in the Z -factor is a signal of a dangerous term with a small energy denominator in the sum of Eq. (24) which determines the $\delta\mu^Z$ and in its counterpart in the sum of Eq. (34) for the $\delta\mu_{GGD}$ term. More exact ac-

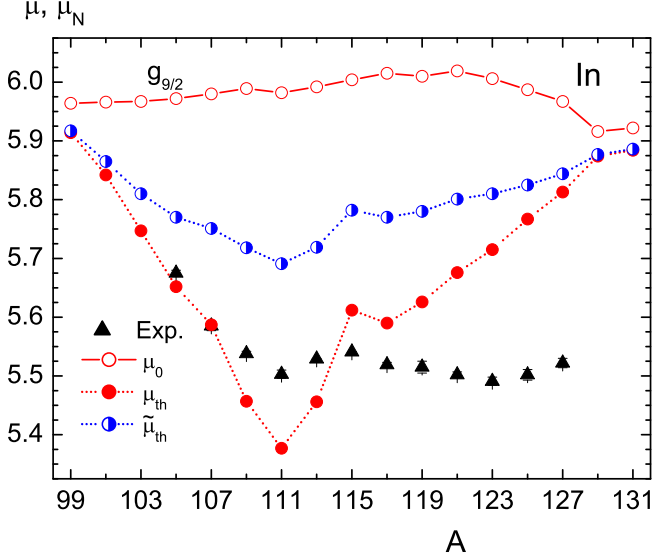


FIG. 23: Magnetic moments of In isotopes.

count for these dangerous contributions is necessary of course. But now we can hope that in so anomalous cases the truth is somewhere between μ_{th} and $\tilde{\mu}_{th}$.

Let us now go to Sb isotopes. Here 4 experimental magnetic moments in the ground states $5/2^+$ of the odd $^{115-121}\text{Sb}$ isotopes are known which correspond to the $2d_{5/2}^p$ particle states and 7 moments for the $1g_{7/2}^p$ state in $^{121-133}\text{Sb}$ isotopes, in the ^{121}Sb isotope we dealing with the first excited state. The total magnetic moments are displayed in Fig. 24 whereas separate PC corrections are represented in Table XIII. For the $1g_{7/2}^p$ state the TFFS without PC corrections describes the data better than for In isotopes discussed above. The maximum of the disagreement, $\simeq 0.3\mu_N$, is for ^{133}Sb . Unfortunately, the PC correction in the vicinity of the magic ^{132}Sn nucleus, just as for neighbors of ^{208}Pb considered previously, is rather small. This correction is rather small also for other isotopes, with exception of two left members of the chain. Here the term $\delta\mu'_{end}$ is bigger than usual and leads to the noticeable value of $\delta\mu_{tot}$. It is worth to mention that the ^{121}Sb nucleus, $\lambda_0 = 1g_{7/2}$, is the only case with positive value of $\delta\mu_{tot}$. As usual, the ansatz $\mu_{th} \rightarrow \tilde{\mu}_{th}$ damps the PC effects, in this case resulting in better agreement with the data.

For $d_{5/2}$ states, the disagreement between TFFS and the data is significant, about $0.6\mu_N$. The size of the PC correction $\delta\mu_{tot}$ is of this order or even bigger. Again the use of the ansatz (54) diminishes the PC effect and again the experimental magnetic moments are between μ_{th} and $\tilde{\mu}_{th}$ values.

Thus, we found that in semi-magic nuclei the PC corrections to the magnetic moments are significant. If we exclude Bi isotopes where they are small, the PC cor-

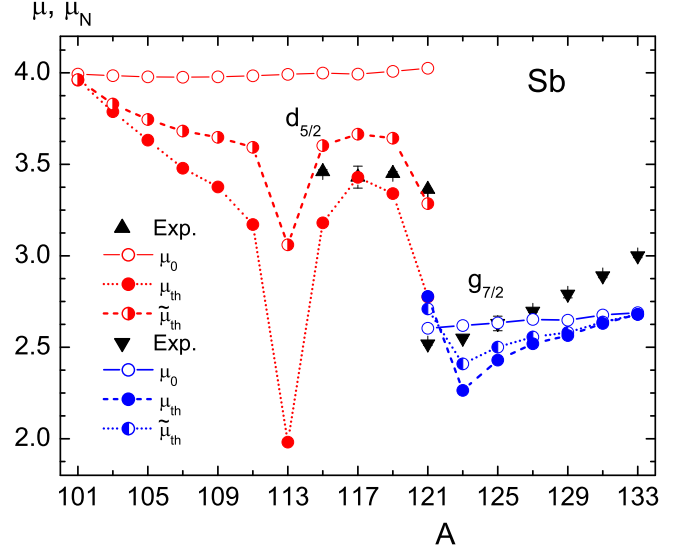


FIG. 24: Magnetic moments of Sb isotopes.

rections have always the sign necessary to improve the agreement with the data.

VIII. CONCLUSION

Within the self-consistent TFFS, we developed a model to calculate the corrections to magnetic moments due to coupling to the low-lying phonons in odd magic and semi-magic nuclei. The main idea of the model is to consider explicitly only those PC diagrams which are sensitive to the nucleus under consideration and the state λ_0 of the odd nucleon. The omitted diagrams are supposed to be included into the universal TFFS parameters.

Among semi-magic nuclei we limit ourselves to those where the odd nucleon belongs to the non-superfluid subsystem. This simplifies the consideration significantly as all PC corrections can be calculated without taking into account the pairing effects. The perturbation theory up to the order of g_L^2 is developed, where g_L is the phonon-particle coupling vertex. The method guarantees the total angular momentum conservation. For this aim, an ansatz is proposed which takes into account the so-called tadpole term.

Three kinds of the PC corrections are considered. The end correction, see Fig. 3, is the first one. The main (pole) part of the end correction, $\delta\mu^Z$, results in \sqrt{Z} -factors on the “ends” of the effective field $V_{\lambda'\lambda}$. The second one denoted as $\delta\mu_{GGD}$, see Fig. 5, describes the effect of the induced interaction due to the L -phonon exchange. The third one labeled as $\delta\mu_{GDD}$, see Fig. 6, describes the effect of the magnetic moment of the phonon. This correction contains two terms of different analytical

TABLE XII: PC contributions to the magnetic moments (in μ_N) of odd In isotopes, $\lambda_0 = 1g_{9/2}$, $L^\pi = 2^+$. The notation is explained in the text nearby Table IV.

A	μ_{exp}	μ_0	$Z(\lambda_0)$	$\delta\mu^Z$	$\delta\mu_{GGD}$	$\delta\mu_{GDD}^{(1)}$	$(\delta\mu_{GDD}^{(2)})$	$\delta\mu'_{\text{end}}$	$\delta\mu_{\text{tot}}$	μ_{th}	$\tilde{\mu}_{\text{th}}$
105	5.675(5)	5.972	0.634	-3.450	2.980	0.155	0.161	-0.002	-0.320	5.652	5.770
107	5.585(8)	5.980	0.584	-4.260	3.680	0.186	0.196	-0.001	-0.393	5.587	5.751
109	5.538(4)	5.989	0.509	-5.770	4.990	0.247	0.263	-0.002	-0.532	5.457	5.718
111	5.503(7)	5.982	0.482	-6.440	5.550	0.286	0.229	-0.002	-0.605	5.377	5.691
113	5.5289(2)	5.992	0.510	-5.770	5.000	0.237	0.257	-0.002	-0.536	5.456	5.719
115	5.5408(2)	6.004	0.609	-3.850	3.330	0.155	0.168	-0.001	-0.364	5.640	5.782
117	5.519(4)	6.016	0.578	-4.390	3.790	0.170	0.184	-0.001	-0.425	5.590	5.770
119	5.515(1)	6.010	0.614	-3.780	3.250	0.160	0.122	-0.001	-0.375	5.635	5.780
121	5.502(5)	6.019	0.634	-3.470	3.000	0.133	0.148	-0.001	-0.343	5.676	5.801
123	5.491(7)	6.006	0.674	-2.900	2.500	0.110	0.123	-0.001	-0.291	5.715	5.801
125	5.502(9)	5.987	0.734	-2.160	1.860	0.081	0.092	0.0	-0.220	5.767	5.826
127	5.522(8)	5.967	0.780	-1.500	1.290	0.055	0.063	0.0	-0.154	5.813	5.844

TABLE XIII: PC contributions to the magnetic moments (in μ_N) of odd Sb isotopes. The notation is explained in the text nearby Table IV.

A	λ_0	μ_{exp}	μ_0	L^π	$Z(\lambda_0)$	$\delta\mu^Z$	$\delta\mu_{GGD}$	$\delta\mu_{GDD}^{(1)}$	$(\delta\mu_{GDD}^{(2)})$	$\delta\mu'_{\text{end}}$	$\delta\mu_{\text{tot}}$	μ_{th}	$\tilde{\mu}_{\text{th}}$
115	$2d_{5/2}$	3.46(1)	3.999	2^+	0.484	-4.260	3.030	0.416	-0.657	0.004	-0.819	3.180	3.602
117	$2d_{5/2}$	3.43(6)	3.993	2^+	0.582	-2.870	2.030	0.274	-0.435	0.002	-0.565	3.429	3.665
119	$2d_{5/2}$	3.45(1)	4.008	2^+	0.547	-3.320	2.350	0.302	-0.479	0.003	-0.668	3.340	3.643
121	$2d_{5/2}$	3.3654(3)	4.025	2^+	0.591	-2.780	1.280	0.252	-0.003	0.002	-1.250	2.775	3.285
121	$1g_{7/2}$	2.518(7)	2.604	2^+	0.607	-1.690	1.440	0.232	-0.224	0.189	0.174	2.778	2.710
123	$1g_{7/2}$	2.5498(2)	2.619	2^+	0.591	-1.810	1.390	0.260	-0.242	-0.191	-0.355	2.264	2.409
125	$1g_{7/2}$	2.63(4)	2.633	2^+	0.651	-1.410	1.080	0.188	-0.182	-0.059	-0.204	2.430	2.501
127	$1g_{7/2}$	2.697(6)	2.652	2^+	0.725	-1.010	0.773	0.127	-0.125	-0.027	-0.133	2.519	2.556
129	$1g_{7/2}$	2.79(2)	2.648	2^+	0.798	-0.670	0.518	0.081	-0.079	-0.012	-0.084	2.564	2.581
131	$1g_{7/2}$	2.89(1)	2.676	2^+	0.836	-0.523	0.391	0.089	-0.057	-0.003	-0.046	2.630	2.638
133	$1g_{7/2}$	3.00(1)	2.689	$2^+ + 3^-$	0.968	-0.087	0.060	0.012	-0.010	0.006	-0.009	2.680	2.680

structure. The term $\delta\mu_{GDD}^{(1)}$ is regular at small phonon excitation energy ω_L whereas the term $\delta\mu_{GDD}^{(2)}$ is singular at $\omega_L \rightarrow 0$. Each of the three types of PC corrections has a tadpole-like counterpart and the one shown in Fig. 7, corresponding to the $\delta\mu_{GDD}$ term, is obviously the most important one. In particular, it possesses the same singularity as the $\delta\mu_{GDD}^{(2)}$ term. We suppose that the sum of tadpole-like terms and the $\delta\mu_{GDD}^{(2)}$ one compensate each other. It is motivated by the observation that such an ansatz leads to the total angular momentum conservation with g_L^2 accuracy.

In magic nuclei, the main PC correction comes from the 3_1^- phonon, whereas in non-magic ones the 2^+ -phonon dominates. The main observation of our calculations is the very strong cancelation of the first two corrections, $\delta\mu^Z$ and $\delta\mu_{GGD}$. The scale of the PC corrections may be characterized with the quantity $(1 - Z)$ which determines directly the term $\delta\mu^Z$. With only one exception, the total correction to the magnetic moment $\delta\mu_{\text{tot}}$ has the same sign as $\delta\mu^Z$, and the absolute value is up to ten times smaller than the individual contributions. As the result of this cancelation, in magic nuclei

where the value of $(1 - Z) \simeq 0.1$ is typical, PC corrections are as a rule negligible. In any case, it is so for all magnetic moments where experimental data exist. In particular, PC corrections can not help to solve the old for the TFFS theory problem of the magnetic moment of the ground state of ^{209}Bi where the theoretical value deviates by $\simeq 0.5 \mu_N$ from the experiment. Evidently, the standard form of the spin-dependent LM amplitude is not sufficient in this case and additional terms including the spin-orbit and tensor in the cross-channel interaction should be taken into account. Thus the problem should be solved at the RPA level.

Simultaneously we calculated the gyromagnetic ratios g_L^{ph} of all low-lying phonons in ^{208}Pb . For the 3_1^- state it is rather close to the BM model prediction $g_L^{\text{ph}} = Z/A$ which is a result of its strong collectivity. Other L -phonons are much less collective and their gyromagnetic ratios strongly differ from the BM ones.

We calculated the PC corrections to four chains proton-odd semi-magic nuclei. The odd Tl and Bi isotopes are the odd neighbors of the even lead isotopes. The Bi chain contains 7 nuclei with known magnetic moment in the same $1h_{9/2}^p$ ground state and the PC cor-

rection $\delta\mu_{\text{tot}}$ is much less than necessary to explain the data in non-magic isotopes too. Evidently, the problem of ^{209}Bi should be solved first at the RPA level which will reduce the disagreement for the whole Bi chain. For Tl isotopes there are 10 isotopes with known magnetic moment in the $3s_{1/2}^{-p}$ ground state. For the magic isotope ^{207}Tl TFFS agrees with the data perfectly well and the PC correction as it was said above is negligible. For non-magic Tl isotopes the typical disagreement is $\simeq 0.2 \mu_N$ and PC corrections reduces it by one half. For odd-proton neighbors of the even tin isotopes, the odd In and Sb chains, the PC effects are stronger than in the lead chain. In such a situation, sometimes the use of the perturbation theory in g_L^2 seems questionable and we suggested the ansatz given in Eq. (54) of an approximate account for the higher order terms in g_L^2 . It corresponds to partial summation of the pole end diagrams in Fig. 3

itself and in the “ends” of Fig. 5 and Fig. 6 as well. This ansatz, $\mu_{\text{th}} \rightarrow \tilde{\mu}_{\text{th}}$, reduces the PC effect that is important in several cases. In general, in both the chains the PC corrections improves the agreement.

IX. ACKNOWLEDGMENT

The work was partly supported by the DFG and RFBR Grants Nos. 436RUS113/994/0-1 and 09-02-91352NNIO-a, by the Grant NSh-215.2012.2 of the Russian Ministry for Science and Education, and by the RFBR Grants 11-02-00467-a, 12-02-00955-a, and 13-02-00085-a. Four of us, E. S., O. A., S. Ka., and S. T., are grateful to the Institut für Kernphysik, Forschungszentrum Jülich for its hospitality.

-
- [1] S. T. Belyev, Mat. Fys. Medd. Dan. Vid. Selsk. **31**, No. 11 (1959).
 - [2] S. Goriely, N. Chamel, and J. M. Pearson, Phys. Rev. Lett. **102**, 152503 (2009).
 - [3] J. Erler, P. Klüpfel, and P.-G. Reinhard, Phys. Rev. C **82**, 044307 (2010).
 - [4] S. Goriely, S. Hilaire, M. Girod, and S. Péru, Phys. Rev. Lett. **102**, 242501 (2009).
 - [5] P. Ring, Prog. Part. Nucl. Phys. **37**, 193 (1996).
 - [6] S. A. Fayans, S. V. Tolokonnikov, E. L. Trykov, and D. Zawischa, Nucl. Phys. A **676**, 49 (2000).
 - [7] V. A. Khodel and E. E. Saperstein, Phys. Rep. **92**, 183 (1982).
 - [8] A. B. Migdal, *Theory of finite Fermi systems and applications to atomic nuclei* (Nauka, Moscow, 1965; Wiley, New York, 1967).
 - [9] S. A. Fayans and V. A. Khodel, JETP Lett. **17**, 444 (1973).
 - [10] S. T. Belyev, A. V. Smirnov, S. V. Tolokonnikov, and S. A. Fayans, Yad. Fiz. **45**, 1263 (1987) [Sov. J. Nucl. Phys. **45**, 783 (1987)].
 - [11] J. Terasaki, J. Engel, and G. F. Bertsch, Phys. Rev. C **78**, 044311 (2008).
 - [12] A. P. Severyukhin, V. V. Voronov, and Nguyen Van Giai, Phys. Rev. C **77**, 024322 (2008).
 - [13] G. F. Bertsch, M. Girod, S. Hilaire, J.-P. Delaroche, H. Goutte, and S. Péru, Phys. Rev. Lett. **99**, 032502 (2007).
 - [14] A. Ansari and P. Ring, Phys. Rev. C **74**, 054313 (2006).
 - [15] S. V. Tolokonnikov, S. Kamerdzhiev, D. Voitenkov, S. Krewald, and E. E. Saperstein, Phys. Rev. C **84**, 064324 (2011).
 - [16] V. G. Soloviev, *Theory of Complex Nuclei*, (Moscow: Nauka, 1971; Oxford: Pergamon Press, 1976).
 - [17] P. F. Bortignon, R. A. Broglia, D. R. Bés, and R. Liotta, Phys. Rep. **30**, 305, 1977.
 - [18] G. Colo, Nguyen Van Giai, P. F. Bortignon, R. A. Broglia, Phys. Rev. C **50**, 1496 (1994).
 - [19] S. Kamerdzhiev, J. Speth, G. Tertychny, Phys. Rep. **393**, 1 (2004).
 - [20] D. Sarchi, P. F. Bortignon, G. Colo, Phys. Lett. **B601**, 27 (2004).
 - [21] V. Tselyaev, Phys. Rev. C **75**, 024306 (2007).
 - [22] A. Avdeenkov, F. Gruemmer, S. Kamerdzhiev *et al.*, Phys. Lett. **B653**, 196 (2007).
 - [23] N. Paar, D. Vretenar, E. Khan, and Gianluca Colo, Rep. Prog. Phys. **70**, 691 (2007).
 - [24] N. Lyutorovich, V. Tselyaev, J. Speth, S. Krewald, F. Grümmer, and P.-G. Reinhard, Phys. Rev. Lett. **109**, 092502 (2012).
 - [25] A. Avdeenkov, S. Goriely, S. Kamerdzhiev, and S. Krewald, Phys. Rev. C **83**, 064316 (2011).
 - [26] N. J. Stone, Atomic Data Nuclear Data Table **90**, (2005) 75.
 - [27] P. Vingerhoets, K. T. Flanagan, and M. Avgoulea, *et al.*, Phys. Rev. C **82**, 064311 (2010).
 - [28] M. Honma, T. Otsuka, B. A. Brown, and T. Mizusaki, Phys. Rev. C **69**, (2004) 034335.
 - [29] I.N. Borzov, E.E. Saperstein, and S.V. Tolokonnikov, Phys. At. Nucl. **71**, 469 (2008).
 - [30] I. N. Borzov, E. E. Saperstein, S. V. Tolokonnikov, G. Neyens, and N. Severijns, Eur. Phys. J. A **45**, 159 (2010).
 - [31] S. V. Tolokonnikov, S. Kamerdzhiev, S. Krewald, E. E. Saperstein, and D. Voitenkov, EPJA **48**, 70 (2012).
 - [32] S. Kamerdzhiev, S. Krewald, S. Tolokonnikov, E. E. Saperstein, and D.Voitenkov. EPJ Web of Conferences **38**, 10002 (2012).
 - [33] D. Voitenkov, S. Kamerdzhiev, S. Krewald, E. E. Saperstein, and S. V. Tolokonnikov. PRC **85**, 054319 (2012).
 - [34] A. V. Smirnov, S. V. Tolokonnikov, and S. A. Fayans, Sov. J. Nucl. Phys. **48**, 995 (1988).
 - [35] S. A. Fayans, JETP Letters **68**, 169 (1998).
 - [36] S. V. Tolokonnikov and E. E. Saperstein, Phys. Atom. Nucl. **73**, 1684 (2010).
 - [37] S. V. Tolokonnikov, S. Kamerdzhiev, S. Krewald, E. E. Saperstein and D. Voitenkov. EPJ Web of Conferences **38**, 04002 (2012).
 - [38] R. Bauer, J. Speth, V. Klemt, P. Ring, E. Werner and T. Yamasaki, Nucl. Phys. A **209**, 535 (1973).
 - [39] V. N. Tkachev, I.N. Borzov, S. P. Kamerdzhiev Sov. J. Nucl. Phys. **24**, 373 (1976).
 - [40] I. N. Borzov, S. V. Tolokonnikov, and S. A. Fayans, Yad. Fiz. **40**, 1151 (1984) [Sov. J. Nucl. Phys. **40**, 732 (1984)].

- [41] I. Hamamoto, Phys. Lett. **B61**, (1973) 343.
- [42] A. P. Platonov, Sov. J. Nucl. Phys. **34**, 342 (1981).
- [43] V. N. Tselyaev, Sov. J. Nucl. Phys. **50**, 780 (1989).
- [44] I. S. Towner, Phys. Rep. **155**, 264 (1987).
- [45] A. P. Platonov and E. E. Saperstein, Nucl. Phys. A **486**, (1988) 63.
- [46] S. Shlomo and G. F. Bertsch, Nucl. Phys. A **243**, (1975) 507.
- [47] J. E. Wise, J. R. Calarco, J. P. Connely, S. A. Fayans, F. W. Hersman, J. H. Heisenberg, R. S. Hicks, W. Kim, T. E. Milliman, R. A. Miskimen, G. A. Peterson, A. P. Platonov, E. E. Saperstein and R. P. Singhal, Phys. Rev. C **47** (1993) 2539.
- [48] A. P. Platonov, E. E. Saperstein, S. V. Tolokonnikov, and S. A. Fayans. Phys. At. Nuc. **58**, 556 (1995).
- [49] A. Bohr and B. R. Mottelson, *Nuclear Structure* (Benjamin, New York, Amsterdam, 1969.), Vol. 1.
- [50] E. E. Saperstein and S. V. Tolokonnikov, JETP Lett. **68**, 553 (1998).
- [51] E. E. Saperstein and S. V. Tolokonnikov, Yad. Fiz. **62**, 1383 (1999) [Phys. Atom. Nucl. **62**, 1302 (1999)].
- [52] A. Bohr and B. R. Mottelson, *Nuclear Structure* (Benjamin, New York, Amsterdam, 1974.), Vol. 2.
- [53] S. P. Kamerzhiev, A. V. Avdeenkov and D. A. Voitenkov, Yad. Fiz. **74**, 1509 (2011) [Phys. Atom. Nucl. **74**, 1478 (2011)].
- [54] S. Kamerzhiev and E. E. Saperstein, Eur. Phys. J. A **37**, 333 (2008).
- [55] S. Kamerzhiev and D. Voitenkov, arXiv:1110.0654 (2011).
- [56] S. P. Kamerzhiev, Sov. J. Nucl. Phys. **38**, 188 (1983).
- [57] V. F. Dmitriev and V. B. Telicin, Nucl. Phys. A **402**, (1983) 581.